

RESERVATIONS CONCERNING THE USE OF "MODEL COMPOUNDS" FOR COALS

John Larsen
Department of Chemistry
Lehigh University
Bethlehem, PA 18015

Keywords: Model compounds, structure, reactivity, macromolecular

INTRODUCTION

A major goal in coal chemistry is understanding the chemical reactions which occur in coals, especially those reactions which occur during coal conversion. One frequently used approach is to study the reaction of compounds which are thought to contain specific functional groups which occur in coals and assume these functional groups will react identically in the coal and in the model system. This paper is an exploration of the "model compound" approach and an attempt to develop criteria for judging the relevance of "model compound" studies to more complex coal systems.

To provide correct insights into the chemistry which occurs during a reaction of a coal, three major criteria must be met: 1) The functional group being studied must exist in coals and its reactivity range in coals due to different substituent effects must be understood and explicitly considered. 2) Knowledge of the reaction environment in the coal must be understood at a level which allows reactivity to be corrected for differences in environment. This includes correcting reactions for "solvent effects". 3) The actual reaction occurring in the coal must be identified and understood. If all these criteria are met, the use of "model compounds" can be a very powerful means for exploring coal reactivity. If even one of the criteria is not met, then the "model compound" study may not provide insight into the chemistry occurring in the coal.

It is my belief that our knowledge of coal structure is sufficiently incomplete to make the routine utilization of model compounds unwise. A wise approach is to identify a reaction which is occurring in coals and then to develop a thorough understanding of that reaction and how it will be altered when it occurs in a coal's macromolecular system. This will involve work with pure compounds, some of which may be, but do not need to be, directly representative of coal structures. Often, the greatest insight into reactions comes from working at the extremes of reactivity. It is much better to understand the reaction thoroughly than it is to carry out an incompletely understood reaction on molecules which are believed to be representative of structures which occur in coals. Once the reaction is understood, attempts can be made to extrapolate this chemistry into the complex macromolecular coal system. In doing this, it is incumbent upon us to explicitly recognize the uncertainties in that extrapolation which derive from our uncertainties about the structure of coals. The work should come full circle. It will start with a study of real coals to identify an important reaction. This stage should be thorough enough to provide certainty as to the identity of that reaction. Then the laboratory or the library is used to gain a mastery of that particular reaction. With a thorough understanding of the reaction in hand, one then moves back to predictions about the

behaviors of coals by considering the effects of the coal medium and structure on the understood reaction, completing the circle.

I will consider briefly our state of knowledge in the three areas I regard as crucial: coal structure, coal as a reaction environment, and our knowledge of the reactions which are actually occurring in coals. My conclusion is that our knowledge in all three areas is sufficiently uncertain to make extrapolations from routine "model compound studies" to coals quite unreliable, and the circular experimental pathway described above is strongly recommended.

Our knowledge of the functional groups which are present in coals has increased enormously, but is still inadequate in some major areas. Consider first our knowledge of the composition of coals. Finseth has recently demonstrated that significant errors in the hydrogen content can derive from incomplete drying of coals under conditions currently in wide use for drying coals.¹ Oxygen content is usually done by difference, a procedure which concentrates all of the errors here. A recent paper compared many different methods for oxygen analysis and showed² that they give divergent results in a non-systematic way. There remain significant problems in the routine determination of the composition of coals. It would be nice to have well checked, very accurate compositional data for all of the Argonne coals which explicitly include consideration of the analytical difficulties.

The oxygen functional group distribution has received much attention. Stock has done a magnificent job in determining the oxygen functional group distribution of Illinois No. 6 coal.³ This was a major research undertaking, and I believe this is the only coal for which a complete and reasonably detailed oxygen functional group distribution has been published. Liotta has published some detailed information on oxygen functional group distribution in a Rawhide (Wyodak subbituminous) coal, and there are attempts to characterize oxygen using NMR spectroscopy without chemical derivatization.^{4,5} This latter work provides no information about substitution patterns, which are important. Stock has provided some information on the number of aromatic rings which have two oxygen functionalities. This seems to be all that is available. This is an important issue because of the possibility of large substituent effects. Important simple questions remain unanswered. What is the distribution of the phenolic hydroxyls or ethers over the different polynuclear aromatic systems? A 9-phenanthryl ether often reacts very differently than does a phenyl ether. What is the size distribution of the alkyl chains in aralkyl ethers? To fully understand the behavior of a functional group, the range of coal structures in which it occurs must be known. NMR techniques to explore the environment of oxygen atoms using cross-polarization are under development.

The introduction of sophisticated NMR techniques has made possible the determination of the range of PNA structures in coals⁶ and this has been done for all of the Argonne premium coals. But, in spite of the advances in NMR, there are still major disagreements about the ring size distributions of the aromatics in coals. Our knowledge of aliphatic structures is not as great. In fact, only recently have definitive structural assignments been made of a majority of the aliphatic carbons in a single coal.⁹ Only recently have there been attempts to quantitatively explore the number of acidic carbon sites

in coals.¹⁰ There are few, if any, functional groups whose population in several coals of varying rank is unquestioned.

Coals are horrendously complex reaction environments. As mined, they are glassy, macromolecular systems containing a complex pore structure.¹¹ Molecular diffusion through glassy materials is very slow and many organic reactions of coals carried out at or near room temperature are mass transport limited.^{4,12} Coals imbibe many solvents and swell in the process. With strongly swelling solvents such as pyridine, the glass-to-rubber transition is suppressed significantly below room temperature and the coals are in a rubbery state.¹³ Diffusion rates in the rubbery state are enhanced by several orders of magnitude over those in the corresponding glass. The rubbery coal is still a macromolecular system which does not dissolve, so the kind of intimate mixing familiar in solution reactions does not occur. The reagent must gain access to the reaction site by diffusing through a rubbery solid. There will usually be significant mass transfer constraints on reactions of coals which involve reagents even if the coals are rubbery.

Even in reactions which do not involve an outside reagent but which are initiated within the coal, mass transport plays a role. If thermal bond homolysis occurs in a coal, the pair of radicals produced may be constrained to stay near each other by large cage effects. If the coal is still glassy, they will not be able to separate rapidly because of the absence of large scale molecular motion. If the coal is rubbery, cage effects will be much less, but the ultimate translational freedom of the radicals will be limited by their position in the coal macromolecular structure. They may not be able to diffuse to their most thermodynamically or kinetically favorable reaction partner, but may be forced by the constraints of the macromolecular system to react with a nearby group. To understand reactions in coals, the environment of the intermediates must be known, at least on a statistical basis. No information of this sort has been published. The very important work of Poutsma, Buchanan and co-workers has demonstrated another pathway for radical diffusion. They have recently shown that radicals can migrate across a plane of molecules bonded to a silica surface by sequential hydrogen abstraction reactions.¹⁴ This is a crucial observation since it provides a mechanism for the rapid diffusion of a reactive center through the coal and justifies ignoring diffusional limitations for a range of radical reactions. Some mechanism of this sort must be involved in the artificial coalification experiments of Winans et al. which are catalyzed by clays, yet which occur throughout the mass of the sample, not just adjacent to the clay surface.¹⁵ Whether the intermediates involved are radicals or ions has not been established.

One other aspect of the macromolecular nature of coal has important effects on reactivity. It is that coals are selective absorbents.¹⁶ While extensive work has been done to model coal reactivity containing good hydrogen donors like tetralin, the composition of the reacting coal in any direct liquefaction process has never been defined. The coal will have been swollen by components from the recycle solvent. It has been documented extensively that coals are selective absorbents,¹⁶⁻¹⁸ and that they do not have a large affinity for aliphatic materials. The reacting coal system will consist of coal and an unknown mixture of components selectively extracted from

the recycle oil, probably in about equal amounts. Modeling coal conversion processes using model compounds will be a fatuous activity until the reacting system has been adequately defined. The same constraints do not apply to pyrolysis reactions, but there cage effects and other mass transport issues become complex and difficult to handle.

The last issue to be discussed is the nature of the reactions which are occurring in coals. There is general agreement that radical reactions are involved in coal conversion. An early simplistic mechanism that the reaction proceeded totally by bond homolysis followed by "capping" of the radicals by hydrogen donors has largely been replaced by the realization that a variety of chain processes are occurring in addition to the simple homolytic bond cleavage.^{19,20} The extent and role of these chain reactions is still an object of much discussion. The family of radical reactions which are occurring still has not been completely elucidated. The use of probe molecules should be a major help.²¹

Radical reactions may not be the only ones occurring. Brower has published impressive evidence based on volumes of activation and isotope effects that ionic and/or electrocyclic processes must be occurring during coal liquefaction.²² I have yet to see a convincing explanation for or rationalization of Brower's data. Ross has recently become concerned with ionic reactions occurring at the coal-mineral matter interface.²³ Much chemistry is possible here as demonstrated by the Winans' coalification experiment. Its role in coal conversion, if any, has not yet been elucidated. Finally, there is the whole question of radical anion and radical cation chemistry.

In summary, there is abundant evidence for the existence of a variety of radical processes occurring during coal conversion. The snarl of competing and parallel reactions has not yet been unraveled. There exists evidence that the principle pathways may not be solely radical reactions, and this evidence has been largely ignored. It seems clear that one must deal with complex radical chemistry when considering coal conversion and coal pyrolysis. Whether radical reactions are the only pathways which must be considered is not yet clear.

Coal is perhaps the most complex organic material whose structure and reactivity has been systematically studied. It is a largely insoluble, black, amorphous, inhomogeneous system containing a wide variety of structural groups and a respectable population of free radicals, and it is not surprising that the progress has been slow and difficult. I believe that achieving the most rapid progress possible requires explicit recognition and acceptance of the enormous complexity of the material. There have been many model compound studies published in which many of the structural complexities are ignored. The use of simplified models and procedures imposes the duty to identify the simplifying assumptions and their potential impact on any conclusions reached.

ACKNOWLEDGEMENT

Grateful acknowledgement is made of the financial support of our efforts in coal chemistry received from the U.S. Department of Energy, the Exxon Education Foundation, and Exxon Research and Engineering Co.

REFERENCES

- (1) Finseth, D. Am. Chem. Soc. Div. Fuel Chem. Prepr. **1987**, 32(4), 260-263.
- (2) Ehmann, W. D.; Koppenaal, D.; Hamrin, C. E. Jr.; Jones, W. C.; Prasad, M. N.; Tian, W.-Z. Fuel **1986**, 65, 1563-1570.
- (3) Stock, L. M.; Willis, R. S. J. Org. Chem. **1985**, 50, 3566-3573.
- (4) Liotta, R.; Brons, G. J. Am. Chem. Soc. **1981**, 103, 1735-1742 and previous papers in this series.
- (5) Dereppe, J.-M.; Moreaux, C.; Landais, P.; Monthieux, M. Fuel **1987**, 66, 594-599 and references therein.
- (6) Hagaman, E. W. Energy Fuel **1988**, 2, 861-862.
- (7) Solum, M. S.; Pugmire, R. J.; Grant, D. M. Energy Fuels **1989**, 3, 187-193.
- (8) Winans, R. E.; Hayatsu, R.; McBeth, R. L. Am. Chem. Soc. Div. Fuel Chem. Prepr. **1988**, 33(1), 407-414.
- (9) Stock, L. M.; Wang, S.-H. Energy Fuels **1988**, 3, 533-535.
- (10) Hagaman, E. W.; Chambers, R. R. Jr.; Woody, M. C. Energy Fuels **1987**, 1, 352-360.
- (11) Coal Structure, Meyers, R. A. Ed., Academic Press; New York: 1982.
- (12) Larsen, J. W.; Green, T.K.; Choudhury, P.; Kuemmerle, E. W. Adv. in Chem. Ser. **1981**, 192, 277-291.
- (13) Brenner, D. Fuel **1985**, 64, 167-173.
- (14) Buchanan, A. C. III; Britt, P. F.; Biggs, C. A. Proc. Intl. Conf. Sci. **1989**, 1, 185-188.
- (15) Hyatsu, R.; McBeth, R. L.; Scott, R. G.; Botto, R. E.; Winans, R. E. Org. Geochem. **1983**, 6, 463-471.
- (16) Whitehurst, D. D.; Mitchell, T. O.; Farcasiu, M.; Coal Liquefaction, Academic Press; New York: 1980, p. 92.
- (17) Hombach, H.-P. Fuel, **1980**, 59, 465-470.
- (18) Green, T. K.; Larsen, J. W.; Fuel, **1984**, 63, 1538-1543.
- (19) Curran, G. P.; Struck, R. T.; Gorin, E. I&EC Proc. Des. Develop. **1967**, 6, 166-173.
- (20) McMillen, D. F.; Malhotra, R.; Nigenda, S. E. Fuel, **1989**, 68, 380-386.
- (21) Bockrath, B. C.; Schroeder, K. T.; Smith, M. R. Energy Fuels **1989**, 3, 268-272.
- (22) Brower, K. R.; Paja, J. J. Org. Chem. **1984**, 49, 3970-3973.
- (23) Ras, D. R., personal communication.

A SEARCH FOR THE RADICAL HYDROGEN TRANSFER PATHWAY IN COAL HYDROLIQUEFACTION.*

Tom Autrey and James A. Franz
Pacific Northwest Laboratory**

INTRODUCTION

It is generally accepted that the formation of petroleum liquids produced in the thermal liquefaction of coal can not be completely explained by simple homolytic cleavage of strong linkages in coal structures. Model compound studies have been employed to elucidate the mechanisms of scission of strong bonds in coal structures and have provided useful information for increasing the efficiency of the coal liquefaction processes (1).

Radical Hydrogen Transfer (RHT), the transfer of a hydrogen atom from a solvent-derived cyclohexadienyl substituted radical to the ipso position of an aryl-alkyl linkage, has been proposed as an important pathway for the cleavage of strong bonds in coal structures during coal liquefaction (2-4). Elegant numerical modeling studies of the scission of diarylmethane model compounds in the presence of a variety of solvent molecules demonstrated that an alternative mechanism for the scission of the strong bonds in these model compounds may be operative that involves cyclohexadienyl-derived solvent molecules rather than free hydrogen atoms. These studies predicted an activation barrier of 18 to 22 kcal/mol for an endothermic transfer of a hydrogen atom from a cyclohexadienyl solvent molecule to the ipso position of a diarylmethane model compound (5-7). Furthermore, these studies have been utilized to predict the efficiencies of hydrogen donor solvents in the liquefaction of coal samples (8,9). The evidence, however, does not preclude other mechanisms involving the cyclohexadienyl solvent molecules. Other possible mechanisms include an addition-transfer-elimination reaction (10) or other, more traditional radical mechanisms that do not require an exotic reaction pathway involving a hydrogen atom carrier donating a hydrogen atom to a closed shell species.

EXPERIMENTAL

The model compound, 3,6-dihydro-3-methoxycarbonyl bibenzyl, 2, was prepared by the following reaction sequence. *m*-bromobenzaldehyde was added to an ether solution of benzyl grignard at room temperature to yield the expected alcohol. The alcohol was converted to the chloride (SOCl_2) and reduced with LiAlH_4 to give *m*-bromobibenzyl. A grignard reagent from *m*-bromobibenzyl was quenched with CO_2 . Following acidic work-up esterification in methanol gave the methyl ester. Birch reduction of the ester yielded our model compound, 2.

Decane solutions of the ester, 2, (10^{-3} M to 10^{-4} M) containing an internal standard for GC product analysis were prepared in quartz tubes. The

* This work was supported by the Office of Basic Energy Sciences, U. S. Department of Energy.

** Pacific Northwest Laboratory is operated for the U. S. Department of Energy by Battelle Memorial Institute under contract OE-AC06-76RLO 1830.

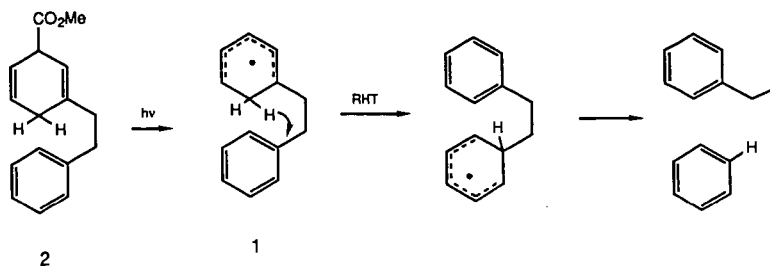
samples were degassed, using three freeze-thaw cycles, and sealed under vacuum. The sealed tubes were irradiated with a high-pressure, 1000-W Hg lamp through the quartz window of a hot air bath, and the temperature was monitored using a thermocouple. Photolysis times ranged from 10 to 15 minutes to yield about 30% decomposition of the starting material. Control experiments showed that the ester was thermally stable under the reaction conditions. Products were analyzed on a HP 5890A GC using on-column injection techniques and were identified by the retention times and GC/mass spectra of authentic compounds.

RESULTS AND DISCUSSION

Our approach to this problem was to design and prepare a new model compound that would provide an unambiguous answer to our question, "What role does Radical Hydrogen Transfer play in the cleavage of strong bonds in coal liquefaction?" We chose a model compound that would provide us with a cyclohexadienyl radical hydrogen donor and an alkyl-phenyl hydrogen acceptor within the same molecule. We anticipated several advantages to this approach in the preparation of our model compound 3,6-dihydro-3-methoxycarbonyl bibenzyl, **2**:

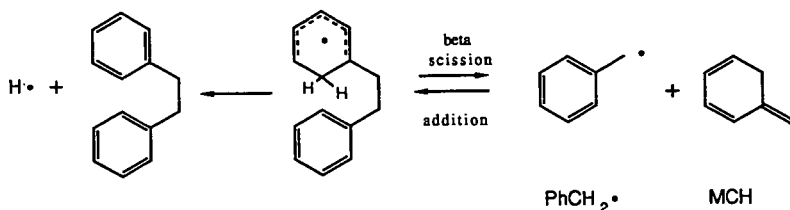
- 1) The cyclohexadienyl transferring agent could conveniently be prepared from a Norrish Type I photo-cleavage of the methyl ester, **1**, at any desirable temperature and at very low rates of initiation favoring unimolecular RHT or scission reactions over bimolecular termination;
- 2) A thermal-neutral hydrogen transfer from a cyclohexadienyl to a phenyl aromatic would provide a lower activation barrier than the endothermic barrier from the numerical modeling studies;
- 3) An intramolecular hydrogen transfer would increase the Arrhenius factor ($\log A$) from 8.5 (bimolecular RHT) to 10 to 11 (intramolecular RHT) thereby suppressing competing side reactions;
- 4) Intramolecular RHT of **1** would proceed through a transition structure of nearly optimal regio- and stereo-chemical orientation, a 1,5 hydrogen migration (11) to yield benzene and phenylethyl radical products as shown in Scheme I;

Scheme I



- 5) A competing β -scission reaction of the cyclohexadienyl radical 1 to yield benzyl radical and methylenecyclohexadiene (MCH) products would provide an internal "clock" to quantify the activation barrier for RHT in this model system as shown in Scheme II;

Scheme II



Irradiation of a dodecane solution containing the methyl ester, 2, (2.4×10^{-4} M) heated to 250 °C in a quartz reactor vessel led to the decomposition of the model compound and the appearance of two cleavage products, toluene (8%) and bibenzyl (24%), yields are based on conversion of starting material. Control experiments showed that the methyl ester was thermally stable under the reaction conditions. Benzene, the RHT product, was not detected.

Irradiation of a concentrated solution of 2 (1.6×10^{-3} M) under the above reaction conditions gave the same products, toluene (3%) and bibenzyl (18%) but no benzene. The decrease in yield of toluene was expected because higher concentrations of benzyl radical lead to an increased rate of termination.

These results require that RHT from the cyclohexadienyl radical to the appended phenyl ring not compete with β -scission of the cyclohexadienyl radical in this model compound, $E_a(\text{RHT}) > E_a(\beta\text{-scission})$. Although we did not observe RHT products in this model system, a lower limit for the activation barrier of a RHT pathway for this system can be determined. This lower limit can be obtained from a calculation of activation barrier for the competing β -scission reaction (Scheme II) determined by Equation [1].

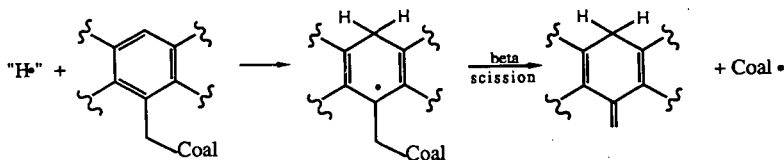
$$E_a = \Delta H_f^\circ(\text{MCH}) + \Delta H_f^\circ(\text{PhCH}_2^\bullet) + E_a(\text{addition}) - \Delta H_f^\circ(1) \quad [1]$$

Only one approximation is necessary in our calculation: The barrier for addition of benzyl radical to methylenecyclohexadiene (MCH), which is the reverse reaction of β -scission. The addition of benzyl radical to styrene was determined to have a barrier of 7 kcal/mol (12). We assume that the barrier for the more exothermic reaction, addition of benzyl radical to MCH, will be no less than 4 kcal/mol. The thermochemical data for the products of the β -scission reaction

were determined previously. We used 48 kcal/mol as the ΔH_f° of benzyl radical (13), and 35 kcal/mol as the ΔH_f° of MCH (14) and we calculated the ΔH_f° of radical 1 to be 60.6 kcal/mol (15). The solution to Equation [1] yields a barrier of 28 ± 3 kcal/mol for β -scission of cyclohexadienyl radical 1 to yield MCH and benzyl radical, just slightly lower than the barrier we calculate for scission of hydrogen atom from a cyclohexadienyl radical ($E_a = 30$ kcal/mol).

It is important to note that this novel β -scission reaction can be responsible for the cleavage of "strong bonds" in coal structures at relatively low temperatures if the appropriate hydrogen atom donors are available. Our new finding suggests that addition of hydrogen atoms to non-ipso ring positions should promote bond cleavage by this β -scission pathway as shown in Scheme III. In this

Scheme III



work β -scission just barely competes with loss of hydrogen ($E_a = 30$ kcal/mol). However, with the addition of hydrogen atoms to larger ring systems the β -scission reaction becomes more important because the barrier for hydrogen loss increases with increasing ring size. When the alkyl linkages are longer than two carbon units the barrier of scission increases, obviously the stability of the radicals produced is a driving force, but β -scission may still compete with loss of hydrogen in larger ring systems. The barrier for β -scission of diarylmethanes is prohibitively high, due to the formation of aryl radicals, and therefore would not have been observed in the numerical model studies.

CONCLUSION

Our examination of the RHT process yields an important result. Our model compound allowed us to "isolate" the RHT process from any competing intermolecular cleavage reaction involving cyclohexadienyl solvent molecules. Our 6-(2-phenylethyl)-cyclohexa-1,3-dien-6-yl radical is consumed by a β -scission pathway, with an activation barrier we calculate to be 28 kcal/mol. No RHT products are observed in our model system. This requires the E_a for RHT to be > 28 kcal/mol, which is substantially higher than the value obtained by the numerical modeling studies (E_a 16 to 22 kcal/mol).

There is convincing evidence that donor solvent structures play an active role, perhaps a predominant role in the cleavage of strong bonds (7-10). In the present work we have conveniently suppressed all side reactions from our

experiments in order to selectively examine the RHT contribution. We do not imply that a RHT pathway does not occur to some extent in the liquefaction of coal, we expect it to have a lower activation barrier than the well-documented Molecular Assisted Homolysis (MAH) reaction (17,18). However, unless significant tunneling of the hydrogen atom through the high barrier (>28 kcal/mol) for RHT occurs, a low activation process responsible for the cleavage of strong bonds in coal structures must occur by an alternative mechanism. The addition-transfer-elimination mechanism (10), a concerted-transfer with elimination pathway (19), and a simple addition-abstraction-elimination reaction pathway are presently being investigated by this group.

REFERENCES

- 1) M. L. Poutsma, A Review of the Thermal Studies of Model Compounds Relevant to Processing Coal, 1987 NTIS Report No. DE88003690/GAR
- 2) D. F. McMillen, W. C. Ogier, S. J. Chang, R. H. Fleming and R. Malhotra, Proceedings of the 1983 International Conference on Coal Science, Pittsburgh, Pennsylvania, 15-19 August, 1983, p. 199.
- 3) R. Billmers, L. L. Griffith and S. E. Stein, J. Phys.Chem. 1986, **90**, 517.
- 4) J. A. Franz, Gordon Research Conference on Free Radical Reactions, June 1981.
- 5) D. F. McMillen, R. Malhotra, S.-J. Chang, and S. E. Nigenda, Am. Chem. Soc., Div. Fuel Chem. Preprints, 1985, **30**(4), 297.
- 6) D. F. McMillen and R. Malhotra, Proceedings of the 1987 International Conference on Coal Science, Maastricht, The Netherlands, 26-30 October, 1987.
- 7) D. F. McMillen, R. Malhotra, S.-J. Chang, W. C. Ogier, E. Nigenda and R. H. Fleming, Fuel, 1987, **66**, 1611.
- 8) D. F. McMillen, R. Malhotra, G. P. Hum and S.-J. Chang, Energy and Fuels, 1987, **1**(2), 193.
- 9) R. Malhotra and D.F. McMillen, Am. Chem. Soc., Div. Fuel Chem. Preprints, 1988, **33**(3), 319.
- 10) R. Billmers, R. L. Brown and S. E. Stein, International J. Chem. Kinetics, 1989, **21**, 375.
- 11) 1,5 Hydrogen atom shifts are the most common. R. K. Freindlina and A. B. Terent'ev, Acc. Chem. Res. 1977, **10**, 9.
- 12) M. L. Poutsma and C. W. Dyer, J. Org. Chem. 1982, **47**, 4903.
- 13) M. Rossi and D. M. Golden, J. Am. Chem. Soc. 1979, **101**, 1230.
- 14) J. E. Bartmess, J. Am. Chem. Soc. 1982, **104**, 335.

- 15) S. W. Benson in Thermochemical Kinetics, 1976, Wiley-interscience. Group additivities were used to calculate the ΔH_f° of the parent cyclohexadienyl compound and a BDE of 73 kcal/mol was used for the ipso hydrogen.
- 16) D. F. McMillen, W. C. Ogier, and D. S. Ross, J. Org. Chem. 1981, 46, 3322.
- 17) J. A. Franz, D. M. Camaioni, R. R. Beishline and D. K. Dalling, J. Org. Chem. 1984, 49, 3563.
- 18) W. D. Graham, J. G. Green and W. A. Pryor, J. Org. Chem. 1979, 44, 907.
- 19) L. M. Tolbert and R. K. Khanna, J. Am. Chem. Soc. 1987, 109, 3477.

ACKNOWLEDGMENT

We thank D. M. Camaioni and C. M. Pollock of the Physical Organic Chemistry Group for sharing the results of their calculations on the concerted transfer mechanism and informing us of Reference (19). This work was supported by the Office of Basic Energy Sciences, U. S. Department of Energy, under contract DE-AC06-76RL0 1830.

KEYWORDS (Radical Hydrogen Transfer, Novel β -scission of Bibenzyl)

THERMOLYTIC CLEAVAGE OF SELECTED ETHER LINKAGES AT MILD TEMPERATURES

Birbal Chawla^{1*}, Burtron H. Davis¹, Buchang Shi², and
Robert D. Guthrie²

¹Center for Applied Energy Research
3572 Iron Works Pike
Lexington, KY 40511

²Department of Chemistry
University of Kentucky
Lexington, KY 40506

INTRODUCTION

Most discussions of coal structure describe the substance as constituted of aromatic, hydroaromatic and heterocyclic aromatic clusters joined by short aliphatic and ether linkages. Various functional groups including phenolic hydroxyl groups and carboxylic acid groups are also present. Because coals are solids with no recognizable repeating units and generally have limited solubility in all solvents, the enterprise of understanding their structures and relating this understanding to practical purposes, necessarily involves some chemical or physical structure disruption with potential loss of information. Most frequently this has involved thermolysis with hydrogen-donor species present. Recently there has been an increased interest in chemical processing which can be carried out under relatively mild conditions (1) which might be hoped to preserve more of the structural features of the initial material.

Analysis of the materials produced by the processing of coal has tended to focus on carbon-carbon bond breaking. Ether linkages, although believed to be present, have not been considered in detail for their potential role in the thermal or chemical reactions of coal under relatively mild conditions. This is surprising in view of the fact that compounds which model the types of ether moieties which might be present in coals are known to undergo pyrolytic scission at temperatures comparable to those of coal liquefaction (2,3). Moreover, benzyl phenyl ether has been shown to promote hydrogen transfer between tetralin and diphenylmethane under thermolysis conditions (4) suggesting an indirect role for ether structural units in facilitating thermolytic liquefaction. A number of radical chain processes have been suggested

*Present Address: Mobil Research and Development Corporation, Paulsboro
Research Laboratory, Paulsboro, NJ 08066

as explanations for carbon-carbon bond breaking (5-7), and these would require an initiating radical such as an oxygen-center radical produced by ether scission.

Most of the reported studies describing the thermolysis of coal model compounds, ethers in particular, have been performed at much higher temperatures than used in coal liquefaction processes. Obviously, conclusions derived from thermolysis at the higher temperatures cannot be applied directly toward understanding of coal dissolution and/or thermolysis processes. Therefore, we initiated studies on the chemistry of thermolysis of four arylmethyl aryl ethers which undergo thermolysis to a significant extent under relatively mild reaction conditions.

EXPERIMENTAL

Thermolysis experiments were performed in evacuated glass ampoules at reaction temperatures of 250°C to 350°C. In a typical thermolysis experiment, about 50 to 150 mg of the material was sealed in an evacuated glass ampoule (0.5 cm x 10 cm). The sealed ampoule was wrapped with steel wool and then inserted in a tubing bomb reactor of about 10-15 ml capacity. The reactor was then immersed in a heated sand bath for the desired reaction time. Typically, it required less than two minutes to reach the desired reaction temperature. At the end of the experiment, the reactor was immersed in a cold sand bath. Once the reactor had come back to ambient temperature, the sealed tube was removed from the reactor and was cut open to recover its contents. For comparison purposes, some of the thermolysis experiments were also conducted by charging the microautoclave reactor directly with 50 to 150 mg of the material. The products were recovered from the glass ampoule or from the reactor using tetrahydrofuran (THF). The THF solutions containing the reaction products were analyzed by GC and GC-MS equipped with SUPERCAP "High Temperature", Al clad fused silica bonded methyl silicone column (15 m x 0.25 mm id, 0.1 μ m film).

Four ethers, namely, α -naphthylmethyl phenyl ether (α -NMPHE), α -benzyl naphthyl ether (α -BNE), β -naphthylmethyl phenyl ether (β -NMPHE) and β -benzyl naphthyl ether (β -BNE) were prepared by procedures reported in the literature (8,9).

RESULTS AND DISCUSSION

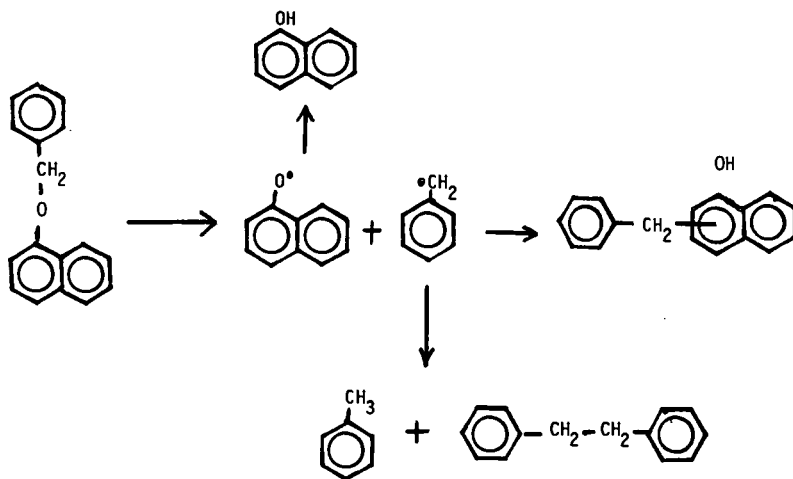
The results of thermolysis of four ethers (α -NMPHE, α -BNE, β -NMPHE, β -BNE) conducted at mild temperatures of 225°C to 350°C with a 30 minute reaction time are given in Table 1 and Figures I and II. Results reported here were calculated based upon the amount of ether left unreacted or decomposed. In order to provide insurance that no appreciable amount of non-volatile product was present, a known amount of triphenylene was added, as an internal standard, during the work up procedure.

As shown by the data in Table 1 and Figures I and II, all the four ethers underwent thermolysis to a significant extent of more than 80% at 325°C or below.

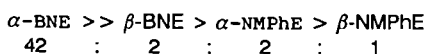
The major products in each case were ArOH, Ar'CH₃, and isomers of the starting ethers which almost certainly have the structures: Ar'CH₂ArOH. Relatively minor amounts of Ar'CH₃CH₂CH₂Ar', Ar'CH=CHAr', Ar'CH₂Ar, and a "dehydrocompound" (parent ion = 232) were also observed. Higher molecular weight materials were found in trace amounts. Isomer yields in sealed tube runs were 30 to 40%, ArOH yields were 20 to 30% and Ar'CH₃ yields were 10 to 30% of GC-observable products.

Formation of observed products could be understood with the help of a typical reaction scheme given below:

THERMOLYSIS OF ALPHA-NAPHTHYL BENZYL ETHER



The relative rates of thermolysis of the four ethers were calculated using the experimental data and were found to be:

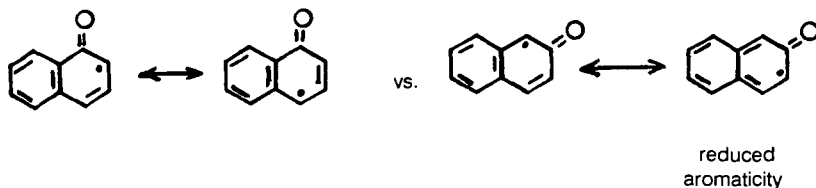


Temp. °C Rate Constant in s⁻¹ x 10⁻⁴ Based on Ether Remaining

	<u>α-BNE</u>	<u>β-BNE</u>	<u>α-NMPHE</u>	<u>β-NMPHE</u>
325	---	17	17	9.4
300	---	2.9	2.3	1.2
285	4.1	0.62	---	0.17
275	7.1	0.34	0.3	---
365	2.6	0.1	---	---

The main conclusion is that the ethers all undergo thermolysis at relatively mild temperatures, presumably by homolysis of the CH₂-O bond followed by recombination of the resultant radicals to give substituted phenols or naphthols or they abstract hydrogen to give ArOH and Ar'CH₃.

An explanation of the relative rates can be found in the relative stabilities of the various radical pairs. Apparently, α -NpCH₂• and β -NpCH₂• differ only slightly in stability whereas α -NpO• is appreciably more stable than β -NpO•. This can be rationalized by assuming that resonance delocalization into the naphthalene ring is much more important in stabilizing NpO• than NpCH₂•. This makes sense because of the instability of oxygen radicals and the strengthening of the C-O bond which results from increasing its C=O character. This analysis also explains why α -NpOCH₂Ph cleaves so much faster than β -NpOCH₂Ph as the α -naphthoxy radical has a contribution of an extra resonance structure:



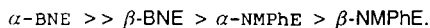
That α -NpOCH₂Ph and β -NpOCH₂Ph should cleave at similar rates is not obvious but the increased stability of α -NpCH₂• relative to PhCH₂• is accidentally equal to the advantage of β -NpO• over PhO•.

A significant difference in product distribution in the thermolysis of α -NMPHE was observed when the reaction vessel was changed from a small glass ampoule (50-150 mg of ether in a 0.5 x 10 cm pyrex ampoule) to a stainless steel pipe reactor (0.5 - 1 g of ether in a 10-15 ml reactor). Relatively larger values of isomers/NpCH₃ + PhOH were observed in the glass vessel. In a previous thermolysis of this ether by Badr and El-Sherief (8) in a sealed glass tube (40 g of ether at 260°C for 7 days), they obtained about the same yield of isomers, but much

more NpCHCH_2Np ($\sim 50\%$). The reasons for these different product distributions are unknown at the present time.

SUMMARY

Thermolysis of four ethers of general structure $\text{Ar}'\text{CH}_2\text{OAr}$, namely, α -naphthylmethyl phenyl ether (α -NMPHE), α -benzyl naphthyl ether (α -BNE), β -naphthylmethyl phenyl ether (β -NMPHE) and β -benzyl naphthyl ether (β -BNE) at mild temperatures of 225°C to 350°C with a 30 minute reaction time was investigated. It was observed that all of the four ethers underwent significant thermolysis to the extent of more than 80% at 325°C or below. The major products in each case were ArOH , $\text{Ar}'\text{CH}_3$, and isomers of the starting ethers. Relatively minor amounts of $\text{Ar}'\text{CH}_2\text{CH}_2\text{Ar}'$, $\text{Ar}'\text{CH}=\text{CHAr}'$, $\text{Ar}'\text{CH}_2\text{Ar}$ and an unknown compound (parent ion = 232) were also observed. Higher molecular weight materials were found in trace amounts. The relative rates of thermolysis were:



ACKNOWLEDGMENT

This research was supported by funds from the U.S. DOE as part of the Consortium for Fossil Fuel Liquefaction Science (CFFLS). Robert D. Guthrie thanks the Research Corporation for a Research Opportunity Award which helped to support the research described above.

REFERENCES

1. (a) Chawla, B.; Davis, B. Prepr. Pap., Am. Chem. Soc., Div. Fuel Chem., **33**, 440, (1988); (b) Keogh, R. A.; Chawla, B.; Tsai, K. J.; Davis, B. H. ibid., 333; (c) Chawla, B.; Keogh, R.; Davis, B. H. ibid., **32**, 324, (1987); (d) Chawla, B.; Davis, B. H. Fuel Sci. and Tech. Int., **7**, 1, (1988); (e) Chawla, B.; Davis, B. H. Fuel Proc. Tech., accepted, (1989); (f) Chawla, B.; Keogh, R.; Davis, B. Energy & Fuels, in press, (1989); (g) Keogh, R.; Poe, S. H.; Chawla, B., in "Coal Science and Technology", Vol. 11, J. A. Moulijn, K. A. Nater, H. A. G. Chermin, eds., Elsevier, New York, 1987, p. 269; (h) Keogh, R.; Klapheke, J.; Poe, S.; Hardy, R.; Taghizadeh, K.; Medina, R.; Taulbee, D.; Chawla, B.; Tsai, K.; Pollock, D.; Hower, J.; Davis, B. Final Report, Contract No. DE-FC22-86PC90017.
2. Chawla, B.; Davis, B. unpublished results.
3. Larsen, J. W.; Keummerle, E. W. Fuel, **55**, 162, (1976).
4. Sharma, D. K.; Mirza, Z. B. Fuel, **63**, 1329, (1984).
5. Reggel, L.; Raymond, R.; Friedman, S.; Friedel, R. A.; Wender, I. Fuel, **37**, 126, (1958).

6. Stock, L. M.; Malya, N.; Willis, R. S. Proc. Int. Conf. Coal Science, 722, 1985.
7. Sternberg, H. W.; Dolle Donne, C. V.; Pentagees, P.; Moroni, E. C.; Markby, R. E. Fuel, 50, 432, (1971).
8. Badr, M. Z. A.; El-Sherief, H. A. H. Indian Journal of Chemistry, 12, 1067, (1974).
9. Maslak, P.; Guthrie, R. D. J. Am. Chem. Soc., 108, 2637-2640, (1986).

Figure 1. Temperature dependence of the extent of conversion of naphthyl methyl phenyl ether (α , \circ ; β , \bullet).

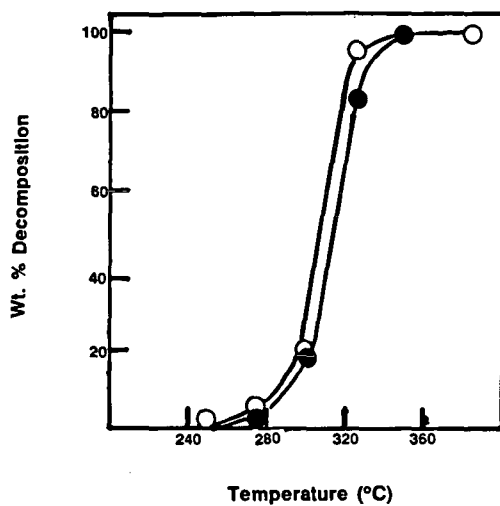
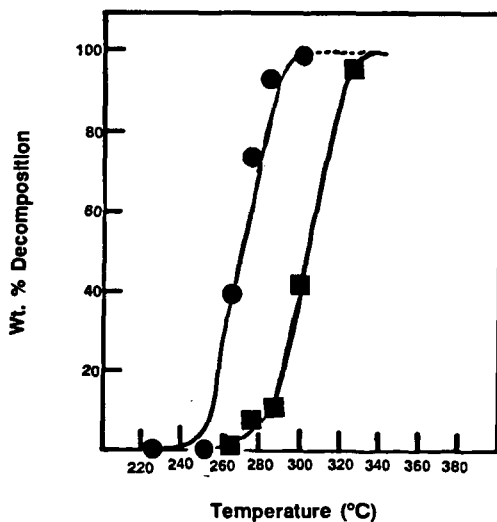


Figure 2. Temperature dependence of the extent of conversion of benzyl naphthyl ether (α , \bullet ; β , \blacksquare).



Pyrolysis of Polycyclic α,ω -Diarylpropanes Pathways, Kinetics, and Mechanisms

C. Michael Smith and Phillip E. Savage
Department of Chemical Engineering
The University of Michigan
Ann Arbor, MI 48109-2136

Division of Fuel Chemistry
Symposium on Model Compounds in Coal Liquefaction
American Chemical Society
Boston, MA Meeting
April 1990

INTRODUCTION

α,ω -Diphenylalkanes have been commonly used as chemical models of the scissile aliphatic linkages between aromatic moieties in coal (e.g., Vernon, 1980; Poutsma and Dyer, 1982; Gilbert and Gajewski, 1982; Sweeting and Wilshire, 1962; Miller and Stein, 1981). In coal, of course, the terminal aromatic moieties are generally neither single ringed nor identical, thus unsymmetrical polycyclic α,ω -diarylalkanes might better mimic these moieties. Studies of these apparently relevant model compounds are few, however. The most probable reason for this gap in the literature stems from the reasoning that the reaction pathways, kinetics, and mechanisms of polycyclic α,ω -diarylalkanes can be extrapolated from those of single ring α,ω -diphenylalkanes. Indeed, the limited previous studies (e.g., Vernon, 1980; Sato, 1979; Javanmardian et al., 1988; Depp et al., 1956) with polycyclic α,ω -diarylalkanes suggest that this premise is reasonable. For example, Javanmardian et al. (1988) reported that the pyrolysis pathway for 2-(3-phenylpropyl)-naphthalene (PPN) led to toluene plus 2-vinylnaphthalene and 2-methylnaphthalene plus styrene; products analogous to those formed during 1,3-diphenylpropane pyrolysis. They further observed approximately equal molar yields of 1-methylnaphthalene and toluene from PPN pyrolysis suggesting that the presence of the naphthyl moiety in a 1,3-diarylalkane had little effect on the selectivity. It did, however, increase the rate of pyrolysis in comparison to that observed for 1,3-diphenylpropane.

In the present work, we further probe the pyrolysis pathways and kinetics of polycyclic α,ω -diarylalkanes. In particular, we present results of pyrolysis studies of two α,ω -diarylpropanes: 2-(3-phenylpropyl)-naphthalene (PPN) and 1,3-bis-(1-pyrene)propane (BPP). This work was motivated by our recent findings that the pyrolysis pathways for *n*-alkyl-substituted pyrenes are markedly different than the pathways for *n*-alkyl-substituted benzenes (Savage et al., 1989; Smith and Savage, 1989). The key differences were the presence of apparent autocatalytic kinetics and the cleavage of the strong aryl-alkyl C-C bond as the pathway to the major products.

EXPERIMENTAL

The pyrolysis of PPN (API Standard Reference Materials) and BPP (Molecular Probes) both neat and in benzene were conducted in constant-volume, 316 stainless steel batch reactors. These reactors were made from one 1/4 in. Swagelok port connector and two 1/4 in. Swagelok end caps and had a volume of $0.59 \pm .05$ ml. For the PPN neat pyrolyses, the batch reactors were loaded with approximately 40 mg of a previously prepared stock solution of PPN and biphenyl (an internal standard), and for BPP neat pyrolyses the batch reactors were loaded with an average of 2.3 mg of BPP and 9.3 mg of biphenyl. For the pyrolyses in benzene, the batch reactors were loaded with approximately 350 mg of a previously prepared stock solution comprising the model compound, biphenyl, and benzene as the inert diluent. All quantities were carefully weighed with an analytical balance. For the pyrolyses in benzene, the reactant concentration was calculated as the number of moles of reactant added to the reactor divided by the reactor volume. After being purged with argon, the reactors were placed in an isothermal fluidized sand bath at the desired temperature (e.g., 400°C). Upon reaching the desired holding time, the reactors were removed from the sand bath and rapidly cooled in an ambient temperature water bath. The reactors were opened, and products were recovered by benzene extraction for BPP and acetone extraction for PPN. Products were identified using GC (HP 5890) and GC-MS (HP 5890 Series II - HP 5970 MSD) and quantified by GC using biphenyl as an internal standard. GC response factors for the reaction products were experimentally determined from standard solutions that contained the reaction products and biphenyl in varying amounts. Plotting the ratio of the mass of a particular compound to the mass of biphenyl in the solution as a function of the ratio of

their integrated GC areas resulted in a straight line and gave the response factor as the slope. The average error for these response factors was 3% (Noggle, 1985).

PPN PYROLYSIS

Experimental Results

Table 1 displays the molar yields of the major products from the neat pyrolysis of PPN at 365 and 400°C and the pyrolysis of PPN in benzene at 375, 400, and 450 °C. The principal products at low PPN conversions were toluene, 2-vinylnaphthalene, 2-methylnaphthalene and styrene, but at high PPN conversions, 2-ethylnaphthalene and ethylbenzene were also present in high yields. The presence of these products and their temporal variations are consistent with the reaction pathway previously determined by Javanmardian et al. (1988). There is, however, a discrepancy with the previous work. Our present work showed that the yields of toluene were higher than the yields of 2-methylnaphthalene, whereas, in the earlier work the yields of toluene and 2-methylnaphthalene were essentially equal. We suspect that the reason for this discrepancy stems from our taking a more careful approach in determining GC response factors for the observed reaction products. Javanmardian et al. (1988) used a single point calibration for the response factors whereas the present analysis used linear regression of at least five points.

The minor products from PPN pyrolysis included 1,3-diphenylpropane and 2-*iso*-propylnaphthalene, which were previously observed by Javanmardian et al. (1988), and naphthalene. The neat pyrolysis also led to the production of acetone-insoluble char. The amounts of this dark solid material increased with temperature and batch holding time. We expect that the formation of this char satisfies the global material balance.

Javanmardian et al. (1988) found that the neat pyrolysis of PPN correlated well with pseudo-first order kinetics. Thus, we calculated pseudo-first-order rate constants from our data and plotted them along with those of Javanmardian et al. (1988) on the Arrhenius plot given as Figure 1. Clearly, the present kinetics results for PPN neat pyrolysis are consistent with the previous work. The Arrhenius parameters determined by Figure 1 are $\log_{10} A = 9.6 \text{ sec}^{-1}$ and $E^* = 38.5 \text{ kcal mol}^{-1}$ for the neat pyrolysis and $\log_{10} A = 7.7 \text{ sec}^{-1}$ and $E^* = 35.2 \text{ kcal mol}^{-1}$ for the pyrolyses in benzene.

Reaction Mechanism

Our results from PPN pyrolysis and previous pyrolyses of its single ring analogue (Poutsma and Dyer, 1982; Gilbert and Gajewski, 1982) led us to propose the free-radical reaction mechanism in Figure 2 to describe PPN pyrolysis. The 18 step mechanism comprises initiation, propagation, and termination steps. Initiation entails the unimolecular dissociation of the weak C-C bonds in the reactant, and we included two possible initiation steps for PPN. The first route corresponds to the formation of benzyl and 2-ethylnaphthyl radicals (denoted β_1 and β_1' in Figure 2), and the second route leads to ethylbenzyl and 2-methylnaphthyl radicals (denoted β_2 and β_2' in Figure 2). Propagation occurs through abstraction of α hydrogens in PPN by β radicals and subsequent β -scission of the resulting radical, μ , to form a stable product Q and regenerate a β radical. Termination of the chain reaction can occur through all possible radical recombination steps.

Kinetics Development

The steady state and long chain approximations can be used to derive an analytical rate expression for the mechanism of Figure 2. The rate of reaction for PPN (denoted as R in Figure 2) is given by Equation 1.

$$-r_R = (k_{11} + k_{12})\beta_1 R + (k_{21} + k_{22})\beta_2 R \quad (1)$$

Expressions for β_1 and β_2 as functions of the rate constants and the reactant concentration can be obtained by writing the long chain rate expressions for β_1 , β_2 , μ_1 , and the total radical population ($R\cdot$). Equations 2-5 display these expressions.

$$r_{\beta_1} = k_{\mu 1} \mu_1 - (k_{11} + k_{12})\beta_1 R = 0 \quad (2)$$

$$r_{\beta_2} = k_{\mu_2}\mu_2 \cdot (k_{21} + k_{22})\beta_2 R = 0 \quad (3)$$

$$r_{\mu_1} = k_{11}\beta_1 R + k_{21}\beta_2 R - k_{\mu_1}\mu_1 = 0 \quad (4)$$

$$r_{R^*} = 2(\alpha_1 + \alpha_2)R - 2\omega_T(\mu_1 + \mu_2 + \beta_1 + \beta_2)^2 = 0 \quad (5)$$

Simultaneous solution of Equations 2-5 provides the required expressions for β_1 and β_2 . These can then be substituted into Equation 1 to derive Equation 6 as the rate law for PPN disappearance.

$$-r_R = \frac{\sqrt{\frac{\alpha_1 + \alpha_2}{\omega_T}} \left[\left(\frac{k_{12}}{k_{21}} \right) (k_{21} + k_{22}) + (k_{11} + k_{12}) \right] R^{3/2}}{\left[\frac{(k_{11} + k_{12})}{k_{\mu_1}} + \left(\frac{k_{12}}{k_{21}} \right) \frac{(k_{21} + k_{22})}{k_{\mu_2}} \right] R + \left[1 + \left(\frac{k_{12}}{k_{21}} \right) \right]} \quad (6)$$

Defining the parameters ζ and ξ as

$$\zeta = \frac{\left[\frac{(k_{11} + k_{12})}{k_{\mu_1}} + \left(\frac{k_{12}}{k_{21}} \right) \frac{(k_{21} + k_{22})}{k_{\mu_2}} \right]}{\sqrt{\frac{\alpha_1 + \alpha_2}{\omega_T}} \left[\left(\frac{k_{12}}{k_{21}} \right) (k_{21} + k_{22}) + (k_{11} + k_{12}) \right]} \quad (7)$$

$$\xi = \frac{\left[1 + \left(\frac{k_{12}}{k_{21}} \right) \right]}{\sqrt{\frac{\alpha_1 + \alpha_2}{\omega_T}} \left[\left(\frac{k_{12}}{k_{21}} \right) (k_{21} + k_{22}) + (k_{11} + k_{12}) \right]} \quad (8)$$

permits the rate law (Equation 6) to be written in more compact form.

$$-r_R = \frac{R^{3/2}}{\zeta R + \xi} \quad (9)$$

Substituting this rate law into the constant volume batch reactor design equation, writing the reactant concentration as a function of conversion (i.e., $R=R_0(1-X)$), integrating, and rearranging, results in a simple expression for the batch holding time (t) as a function of conversion (X) and the initial PPN concentration (R_0).

$$t = \frac{2\xi}{\sqrt{R_0}} \left[\frac{1}{\sqrt{1-X}} - 1 \right] - 2\zeta\sqrt{R_0} \left[\sqrt{1-X} - 1 \right] \quad (10)$$

The mechanism of Figure 2 also permits derivation of an analytical expression for the product selectivity. The instantaneous selectivity (S) of PPN to toluene relative to 2-methynaphthalene is given as the ratio of the reaction rates.

$$S = \frac{r_{\text{TOL}}}{r_{\text{2-MN}}} = \frac{(k_{11} + k_{12}) \beta_1}{(k_{21} + k_{22}) \beta_2} \quad (11)$$

Substituting the relationship between β_1 and β_2 that results from the solution of Equations 2-5 into Equation 11 leads to Equation 12 for the instantaneous selectivity.

$$S = \frac{r_{\text{TOL}}}{r_{\text{2-MN}}} = \frac{\left(1 + \frac{k_{11}}{k_{12}}\right)}{\left(1 + \frac{k_{22}}{k_{21}}\right)} \quad (12)$$

Rate Constant Estimation

Employing Equations 10 and 12 to model the kinetics and selectivity of PPN pyrolysis requires values for each of the rate constants in the reaction mechanism shown in Figure 2. In the following paragraphs we describe our rate constant estimation procedures. Note that the values we used for the rate constants were semi-quantitative. More accurate estimates could be made using thermochemical kinetics.

Rate constants for initiation via homolytic dissociation of C-C bonds typically have pre-exponential factors in the range of $10^{16 \pm 1} \text{ s}^{-1}$ (Benson, 1976). Thus, we selected a value of $A = 10^{16} \text{ s}^{-1}$ for both of the initiation rate constants α_1 and α_2 . We used 69 kcal mol^{-1} as the activation energy for α_1 (which produces a benzyl and 2-ethylnaphthyl radical). This value is in good accord with the calculated bond dissociation energy (BDE) of $68.81 \text{ kcal mol}^{-1}$ for the identical bond in 1,3-diphenylpropane (King and Stock, 1984). The rate of initiation via step α_2 will be faster than via step α_1 because the additional resonance stabilization energy associated with the naphthyl moiety reduces the BDE of the benzylic C-C bond. Thus, the activation energy for this step was taken to be $E^* = 69 - \Delta \text{RSE}$, where ΔRSE is the difference in the resonance stabilization energies between a 2-methylnaphthyl radical and a benzyl radical. We used Sato's calculated value of $0.41 \text{ kcal mol}^{-1}$ for the ΔRSE .

Hydrogen abstraction rate constants were estimated by first assuming that the pre-exponential factors for k_{11} , k_{12} , k_{21} , and k_{22} were all equal to $A = 10^8 \text{ l mol}^{-1} \text{ s}^{-1}$ and that the activation energy for k_{12} was $14.2 \text{ kcal mol}^{-1}$. These Arrhenius parameters for k_{12} are identical to those estimated by Poutsma and Dyer (1982) for abstraction of a secondary benzylic hydrogen by a primary benzyl radical. The activation energy for k_{21} was also taken as $14.2 \text{ kcal mol}^{-1}$ because the reduction in rate for this step relative to k_{12} due to the increased stability of the abstracting radical (i.e., 2-methylnaphthyl vs. benzyl) should be roughly offset by the increase in rate due to the lower C-H bond strength of the β -position being attacked. Finally the activation energies for k_{11} and k_{22} were estimated from the activation energies for k_{21} and k_{12} by assuming that half of the ΔRSE associated with the two different hydrogens being abstracted radicals would appear as the activation energy difference. This is essentially the same as employing the Evans-Polanyi relation with $\alpha=0.5$, a value commonly used (Stein, 1985; Poutsma and Dyer, 1982) for hydrogen abstraction reactions.

Poutsma and Dyer (1982) estimated the Arrhenius parameters for β -scission of an α -radical in 1,3-diphenylpropane to be $A = 10^{14.8} \text{ s}^{-1}$ and $E^* = 28.3 \text{ kcal mol}^{-1}$. For PPN pyrolysis, we expect $k_{\mu 1}$ to be lower than the β -scission rate constant for 1,3-diphenylpropane pyrolysis because the μ_1 radical should be more stable than the corresponding 1,3-diphenylpropane-derived radical. On the other hand, we expect $k_{\mu 2}$ to be higher because the additional RSE due to the presence of the naphthyl moiety in PPN results in the β -scission of a weaker C-C bond. We quantified the foregoing qualitative arguments by taking $10^{14.8} \text{ s}^{-1}$ as the pre-exponential factor for the β -scission steps and using $28.2 \text{ kcal mol}^{-1}$ as the activation energy for $k_{\mu 1}$ and $28.4 \text{ kcal mol}^{-1}$ as E^* for $k_{\mu 2}$.

Termination rate constants for radical recombination generally have zero activation energy and pre-exponential factors of $A = 10^{9.0 \pm 1} \text{ l mol}^{-1} \text{ s}^{-1}$ (Benson, 1976). For our termination rate constant, ω_T , we used $A = 10^{8.5}$ and $E^* = 0.0 \text{ kcal mol}^{-1}$.

Modeling Results

We used the semi-quantitative rate constant estimates described above as parameters in Equations 10 and 12 to calculate the kinetics and selectivity for PPN pyrolysis under the conditions at which we had performed experiments. Figure 3 compares the calculated and experimentally determined temporal variation of the PPN molar yield for the pyrolyses in benzene. Clearly, the kinetics predicted from the reaction model are in good agreement with the experimental data. Figure 4 provides the calculated and experimentally determined instantaneous selectivity of PPN to toluene relative to 2-methylnaphthalene. The data points were calculated as the mean values for all batch holding times at a given temperature. Once again, we find satisfactory agreement between the results of the reaction model and the experiments.

BPP PYROLYSIS

Experimental Results

Table 2 provides the molar yields of the major products from the pyrolysis of BPP neat at 365°C and in benzene at 400°C. The major products from pyrolysis in benzene at short batch holding times (e.g., 10 min), were 1-methylpyrene and 1-vinylpyrene. At long times, however, the yield of 1-vinylpyrene decreased while the yield of 1-ethylpyrene increased. Additionally, pyrene became a major product at the longer holding times. Figure 5, which presents the temporal variations of the product yields for BPP pyrolyses in benzene, displays these trends more clearly.

The neat pyrolysis of BPP led to 1-methylpyrene, 1-ethylpyrene, and pyrene as principal products. No vinylpyrene was detected, but trace amounts of 1-propylpyrene and 1-allylpyrene were observed along with visible amounts of benzene-insoluble char. At a batch holding time of 90 minutes the respective molar yields for 1-methylpyrene, 1-ethylpyrene, and pyrene were 62%, 40% and 23% respectively.

Reaction Pathway

The initial products formed from BPP pyrolysis were 1-methylpyrene and 1-vinylpyrene. These are analogous to toluene and styrene, the primary products of 1,3-diphenylpropane pyrolysis. The coincidence of initial products indicates that the pathway for BPP pyrolysis at short times is identical to the pyrolysis pathway for its single ring analogue, 1,3-diphenylpropane. At longer times and higher concentrations, however, the pyrolysis of BPP led to the formation of appreciable yields ($\geq 30\%$) of pyrene. Similarly high yields of benzene have never been observed from 1,3-diphenylpropane pyrolysis. The pathways responsible for pyrene formation can be inferred from the temporal variations of the product yields illustrated in Figure 5. The molar yields of methylpyrene and ethylpyrene both decreased at the longer holding times where the molar yield of pyrene increased. Thus, it appears that ethylpyrene and methylpyrene underwent secondary reactions that resulted in the loss of their alkyl substituents at the aromatic ring. Such a pathway is entirely consistent with our recent studies of 1-dodecylpyrene pyrolysis (Savage et al., 1989; Smith and Savage 1989) where aryl-alkyl C-C bond cleavage was an important reaction pathway. The amount of pyrene formed, however, may be too high to be the sole result of secondary decomposition reactions of methyl- and ethylpyrene. This suggests that BPP itself may have undergone primary reaction to form pyrene. The precise mechanism for these pathways involving cleavage of strong aryl-alkyl C-C bonds is currently unknown, although the literature does provide some possibilities (e.g., Vernon, 1980; McMillen et al., 1987). Indeed, our earlier work with 1-dodecylpyrene pyrolysis (Smith and Savage, 1989) suggests that radical hydrogen transfer may be responsible for the cleavage of the strong aryl-alkyl C-C bonds during alkyl-pyrene pyrolysis. Figure 6 summarizes the foregoing discussion by displaying the postulated pyrolysis pathways for BPP. Note that the presence of pathways involving aryl-alkyl bond cleavage is a completely new feature of α,ω -diarylpropane pyrolysis.

CONCLUSIONS

1. The pyrolysis pathways for α,ω -diarylkalkanes and hence the corresponding moieties in coal have not been completely elucidated. BPP, a polycyclic diarylkalkanes, followed a pyrolysis pathway where strong aryl-alkyl C-C bonds were cleaved. This appearance of this new pathway clearly

indicates that the complete pyrolytic behavior of α,ω -diarylpropanes can not always be inferred from 1,3-diphenylpropane.

2. For the pyrolysis of PPN, aryl-alkyl cleavage was not a major pathway. The pathways and mechanisms for PPN pyrolysis can be inferred from knowledge of 1,3 diphenylpropane pyrolysis. Furthermore, the reaction kinetics and product selectivities can be accurately calculated for by the accounting for the relevant resonance stabilization energy differences.

NOTATION

A	pre-exponential factor, (l/s, l/mol-s)
E°	activation energy, (kcal/mol)
$k_{\mu i}$	β -scission rate constant, (l/s)
k_{ij}	hydrogen abstraction rate constant, (l/mol-s)
Q	reaction product in Figure 2
r	reaction rate, (mol/l-s)
R	reactant in Figure 2 or reactant concentration, (mol/l)
R_0	initial reactant concentration, (mol/l)
t	batch holding time, (s)
X	reactant conversion
α_i	initiation rate constant, (l/s)
β_i	radical reacting in bimolecular propagation step
$\beta_i H$	stable product in Figure 2, (mol/l)
μ_i	radical reacting in unimolecular propagation step
ζ, ξ	parameters in equation 10
ω_T	termination rate constant, (l/mol-s)

LITERATURE CITED

- Benson, S. W. Thermochemical Kinetics John Wiley and Sons, New York, 1976.
- Depp, E. A., Stevens, C. M., Neuworth, M. B. Pyrolysis of Bituminous Coal Models *Fuel*, 1956, 35, 437.
- Gilbert, K.E., Gajewski, J. J. Coal Liquefaction Model Studies: Free Radical Chain Decomposition of Diphenylpropane, Dibenzyl Ether, and Phenyl Ether via β -Scission Reactions. *J. Org. Chem.*, 1982, 47, 4899.
- Javanmardian, M., Smith, P.J., Savage, P. E. Pyrolysis of Compounds Containing Polycyclic Aromatic Moieties. *Prepr.-Am. Chem. Soc., Div. Fuel. Chem.* 1988,33,242.
- King, H., Stock, L.M. Aspects of the Chemistry of Donor Solvent Coal Dissolution *Fuel*, 1984, 63, 810.
- McMillen, D. F., Malhorta, R., Chang, S.J., Olgier, W.C., Nigenda, E, Fleming, R. H. Mechanisms of Hydrogen Transfer and Bond Scission of Strongly Bonded Coal Structures in Donor-Solvent Systems. *Fuel*, 1987, 66, 1611.
- Miller, R. E., Stein, S. E. Liquid-Phase Pyrolysis of 1,2 Diphenylethane, *J. Phys. Chem.*, 1982, 580.
- Noggle, J. H. Physical Chemistry Little, Brown, and Company, Boston 1985.

Poutsma, M. L., Dyer, C. W. Thermolysis of Model Compounds for Coal. 3. Radical Chain Decomposition of 1,3-Diphenylpropane and 1,4-Diphenylbutane, *J. Org. Chem.*, 1982, 47, 4903.

Sato, Y. Dissociation Energies of C-C Bonds in Bibenzyl and 1,2-di-1-Naphthylethane *Fuel*, 1979, 58, 318

Savage, P.E., Jacobs, G.E., Javanmardian, M. Autocatalysis and Aryl-Alkyl Bond Cleavage in 1-Dodecylpyrene Pyrolysis *Ind. Eng. Chem. Res.*, 1989, 28, 645.

Smith, C. M., Savage, P. E. Pyrolysis of Alkyl-Substituted Polycyclic Aromatic Compounds Paper 93d Presented at AIChE Annual Meeting, San Francisco, CA November, 1989.

Stein, S. E. Free Radicals in Coal Conversion in Chemistry of Coal Conversion, Edited by Richard Scholsberg, 1985, 13.

Sweeting, J. W., Wilshire, J. F. K. The pyrolysis of $\omega\omega'$ -Diphenylalkanes *Aust. J. Chem.*, 1962, 15, 89.

Vernon, L. W. Free Radical Chemistry of Coal Liquefaction: Role of Molecular Hydrogen *Fuel*, 1980, 59, 102.

ACKNOWLEDGEMENTS

This work was supported, in part, by the Shell Faculty Career Initiation Fund, an Energy Research Grant from the University of Michigan Office of the Vice President for Research, and the National Science Foundation (Grant No. CTS-8906859)

Table 1: Summary of PPN Pyrolysis Data
Molar Yields (%) of Products at Different Reaction Conditions

Time	Temp. °C	Conditions	TOL	STY	EB	MN	EN	VN	PPN
40	365	Neat	17.4	4.9	1.5	14.4	2.3	2.2	53.2
40	365	Neat	18.0	4.6	1.6	15.0	2.5	2.2	52.8
46	365	Neat	19.0	4.4	2.1	16.9	3.3	2.0	46.4
76	365	Neat	30.1	3.2	4.9	24.9	6.8	1.5	26.7
99	365	Neat	39.0	0.8	3.1	29.8	10.1	1.1	19.2
158	365	Neat	49.0	1.0	16.3	35.9	17.5	0.5	8.0
11	400	Neat	17.1	8.9	1.4	16.5	2.7	4.5	49.9
17	400	Neat	29.3	9.4	4.7	28.0	7.7	3.3	22.9
31	400	Neat	49.1	3.2	13.2	37.3	15.2	1.2	6.6
47	400	Neat	52.5	1.3	18.1	40.3	18.7	0.0	5.9
105	400	Neat	61.0	0.0	23.3	41.9	19.7	0.0	0.0
151	400	Neat	61.5	0.0	24.3	41.9	19.7	0.0	0.0
10	375	0.12 M Benzene	0.7	0.7	0.0	0.6	0.0	1.0	98.7
30	375	0.12 M Benzene	1.8	1.5	0.0	1.5	0.0	2.2	97.5
60	375	0.12 M Benzene	3.4	2.6	0.0	2.9	0.3	3.8	93.9
95	375	0.12 M Benzene	6.5	4.9	0.4	5.6	1.1	6.8	84.5
150	375	0.12 M Benzene	10.0	7.3	0.7	9.2	1.7	9.4	76.1
240	375	0.12 M Benzene	24.5	11.9	3.6	23.3	7.1	11.7	42.3
20	400	0.12 M Benzene	4.4	3.4	0.0	3.6	0.4	4.8	88.3
30	400	0.12 M Benzene	11.9	8.1	1.3	10.0	2.7	9.6	71.1
45	400	0.12 M Benzene	13.0	9.1	1.1	11.2	2.0	11.3	68.5
60	400	0.12 M Benzene	17.5	11.8	1.6	15.2	2.9	14.2	58.4
60	400	0.12 M Benzene	24.6	11.8	4.9	21.1	8.7	11.7	41.3
90	400	0.12 M Benzene	22.2	13.1	2.6	19.8	4.8	14.4	47.7
150	400	0.12 M Benzene	35.6	9.3	8.4	32.5	12.6	8.2	17.1
153	400	0.12 M Benzene	32.8	9.9	7.4	29.7	11.3	9.1	23.3
10	450	0.12 M Benzene	9.1	6.9	0.7	7.9	1.2	9.7	77.0
15	450	0.12 M Benzene	20.8	12.6	2.6	19.2	4.1	16.5	46.6
30	450	0.12 M Benzene	32.6	9.5	8.7	30.3	12.5	9.9	12.9
45	450	0.12 M Benzene	34.7	9.3	10.6	31.4	16.0	8.9	6.7
60	450	0.12 M Benzene	34.9	0.7	15.8	31.1	18.8	0.6	1.2
90	450	0.12 M Benzene	35.2	0.6	15.0	31.1	18.5	0.5	0.7

Table 2: Summary of BPP Pyrolysis Data
Molar Yields(%) of Products at Different Reaction Conditions

Time	Temp. °C	Conditions	Pyrene	Methylpyrene	Ethylpyrene	Vinylpyrene
10	365	Neat	5.5	34.1	23.9	
20	365	Neat	9.1	43.5	31.1	
40	365	Neat	16.7	58.1	40.9	
50	365	Neat	17.2	63.4	45.4	
90	365	Neat	23.0	61.7	39.6	
155	365	Neat	25.9	52.3	29.9	
10	400	0.005 in Benzene	0.8	3.7	2.3	5.9
20	400	0.005 in Benzene	1.4	10.4	8.2	7.0
30	400	0.005 in Benzene	2.0	15.7	12.0	7.1
45	400	0.005 in Benzene	1.6	15.9	11.4	7.1
60	400	0.005 in Benzene	4.0	35.5	31.0	7.6
120	400	0.005 in Benzene	7.7	51.2	48.5	3.5
180	400	0.005 in Benzene	11.6	56.2	54.3	1.2
240	400	0.005 in Benzene	16.0	62.9	58.3	0.0
411	400	0.005 in Benzene	23.9	60.8	53.4	0.0
816	400	0.005 in Benzene	36.0	42.1	34.2	0.0

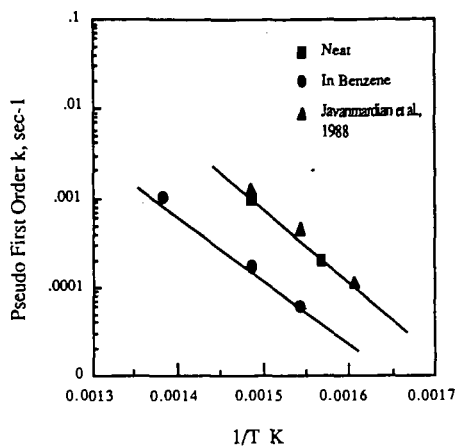


Figure 1: Arrhenius Plot for PPN Pyrolysis

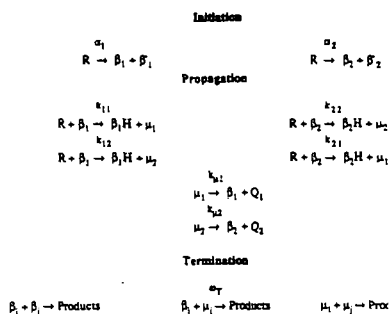


Figure 2: PPN Reaction Mechanism

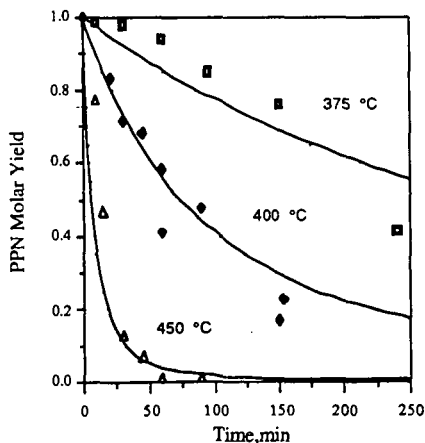


Figure 3: Modeling and Experimental Results for PPN Pyrolysis in Benzene 0.12M

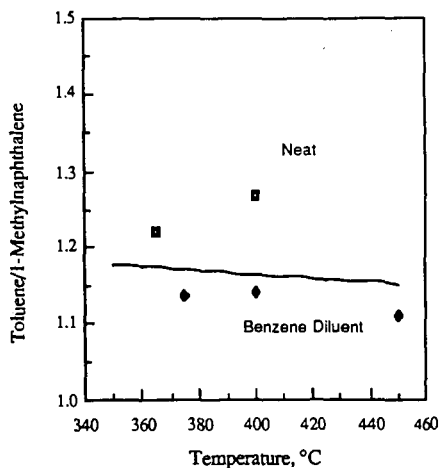


Figure 4: Model Predictions for PPN Pyrolysis Selectivity

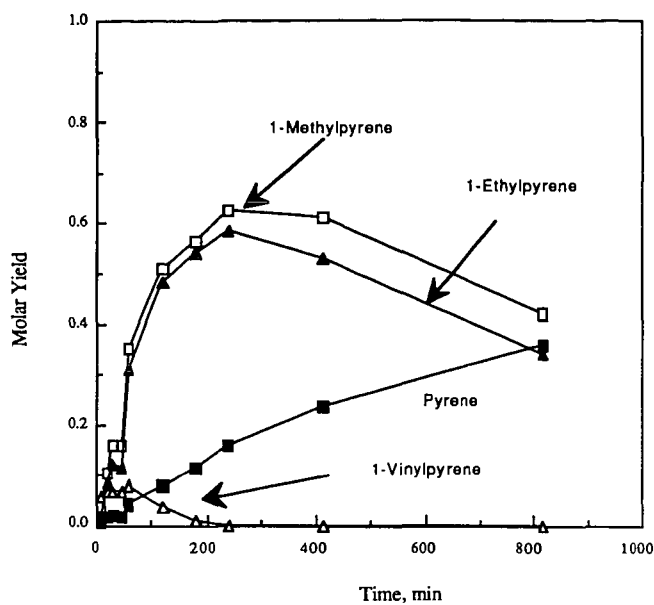


Figure 5: Molar Yields of Major Products for BPP Pyrolysis in Benzene (0.005 M, 400°C)

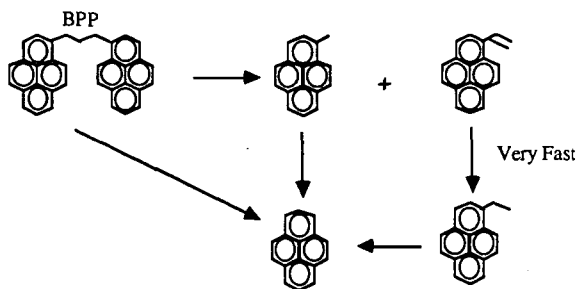


Figure 6: BPP Pyrolysis Pathway

MODELING COAL LIQUEFACTION: DECOMPOSITION OF
4-(1-NAPHTHYLMETHYL)BIBENZYL CATALYZED BY CARBON BLACK*

Malvina Farcasiu and Charlene Smith**
Pittsburgh Energy Technology Center
U.S. Department of Energy
P.O. Box 10940
Pittsburgh, PA 15236

*Reference in the paper to any specific commercial product, process, or service is to facilitate understanding and does not necessarily imply its endorsement or favoring by the United States Department of Energy.

**Oak Ridge Associated Universities Appointee, Postgraduate Research Training Program.

Keywords: coal liquefaction, modeling, carbon black

ABSTRACT

The early stages of coal liquefaction involve cleavage of methylene and ethylene bridges connecting aromatic rings. We modeled this process by the reaction of 4-(1-naphthylmethyl)bibenzyl (I) in the presence of a hydrogen donor (9,10-dihydrophenanthrene). The reactions were conducted over a range of temperatures (320-430°C) and reaction times (30-90 min). We found that the bond between the methylene group and the naphthalene ring and the methylene to methylene bond of the bibenzyl moiety are broken with equal probability. Addition of carbon black (BP 2000) as catalyst (2-10%) increases significantly the conversion of I. For instance, at 419°C and 1h, 18% of I is converted without catalyst and 42% is converted in the presence of 2% of BP 2000. The increase in conversion is due to additional breaking of the bond between the naphthyl and the methylene groups. This particular carbon black is, therefore, a very active and selective catalyst for the cleavage of the naphthyl-to-methylene bond.

INTRODUCTION

Cleavage of covalent bonds is the essential reaction occurring during coal liquefaction. Thermal cleavage requires temperatures so high, that other, mostly undesirable reactions take place resulting in little if any selectivity in the cleavage process. However, specific bonds can be cleaved catalytically, at temperatures where thermal reactions are not important.

Because of the complexity of coal structure, it is not possible to investigate and optimize conditions for cleaving specific bonds, or to sort out desired processes from side-reactions. In order to obtain meaningful data relevant to coal liquefaction and to be able to develop proper catalysts for the process, the study of model compounds containing the critical structural elements of coal in simpler structures is necessary. The study of appropriate model compounds allows determinations of kinetic parameters (rates, activation energies, selectivities) that can be applicable to the cleavage of specific bonds in coal.

To be relevant to coal liquefaction under heterogeneous catalysis, a study of model compounds should satisfy a number of requirements concerning the structure of the model compound, and the type of data to be gathered. Some of these criteria are:

1. The model compound should be liquid or solid under the reaction conditions to mimic the conditions prevalent during coal liquefaction.

This usually means that the model compound should have a molecular weight of at least 300. A macromolecular structure could be desirable in some cases.

2. The model compound should contain several types of potentially reactive chemical bonds under the reaction conditions. The presence of different reactive structures in the same molecule permits the study of competitive kinetics in the presence of intramolecular interactions. Many of the reactions taking place during coal liquefaction are influenced by other chemical structures present in the same molecule. Because competitive reactions certainly occur in coal processing, study of model compounds with only one type of bond that cleaves affords only limited information.
3. The products of reactions should be unambiguously identified and their rate of formation determined. Determination of rates (both absolute and relative) and of activation energies of different reactions is essential for the study of the mechanisms of reactions. Relative reaction rates and activation energies for cleavage of specific bonds is necessary information that cannot be obtained directly from the study of very complex systems such as coal. In the latter case only an overall conversion of a complex starting material to a complex product mixture can be determined. An attempt at calculating an activation energy for such a transformation gives a number with no physico-chemical meaning. In these cases the use of appropriate model compounds is highly desirable.

In the current study, we examined the cleavage of methylene and ethylene bonds linking aromatic fragments. These particular reactions are considered important for the chemistry of coal liquefaction (1). The model compound investigated, 4-(1-naphthylmethyl)biphenyl (I), contains a methylene and ethylene linkage in the same molecule. Thermal as well as catalytic cleavage of the bonds were studied. A novel catalyst was employed (carbon black, Cabot Corporation Black Pearls 2000) for the catalytic reactions. This material has been used as support for metal-based catalysts (2), but has never been reported to be a catalyst itself.

EXPERIMENTAL SECTION

Materials and Analytical Procedures. 9,10-Dihydrophenanthrene was obtained from Aldrich Chemical Co., Black Pearls 2000 carbon black was obtained from Cabot Corporation. Elemental analysis of the carbon black, performed by Huffman Laboratories, Golden, CO, gave % C, 95.4; O, 1.4; S, 1.8; Ash, 1.3. Surface area (BET) quoted by Cabot is 1475 m²/g. 4-(1-naphthylmethyl)biphenyl (I) was prepared in the laboratory of Prof. Paul Dowd at the University of Pittsburgh. The compound was completely characterized by IR, UV, ¹H NMR, ¹³C NMR, elemental analysis and high and low resolution mass spectroscopy. The purity of the product was better than 99%. The above substances were used as received. Dichloromethane was stored over 4 Å molecular sieves.

Glass reaction tubes were made from Pyrex tubing, 5 x 7 mm (i.d. x o.d.). Sealed sample tubes were approximately 75 mm in length.

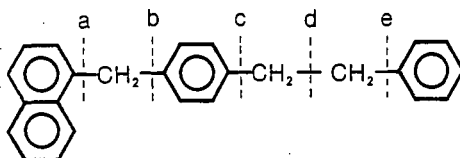
Gas chromatographic analyses were carried out on a Hewlett Packard Model 5730A gas chromatograph equipped with an SE-30 60 m column. Gas chromatography/mass spectra (GC/MS) were obtained on a Hewlett Packard GC/MS Model 5985 instrument operated using 70 eV electron impact voltage and equipped with a 30 m SE-52 column.

Identification of reaction products was accomplished by GC/MS analysis and, when possible, by GC comparison with authentic chemical samples. Reported products yields and overall conversion of I are based on GC measurements. The most volatile material, toluene, could not be determined accurately, but the quantity was always found to be close to that of naphthyl tolyl methane. The amount of toluene reported was set to equal the amount of naphthyl tolyl methane found.

General Experimental Procedure. The reaction components (9,10-dihydro-phenanthrene, ca. 100 mg; I, ca. 25 mg and carbon black, 0, 2, 5, 10 wt % based on I) were weighed into an open-ended glass reaction tube. The tubes were flame sealed, taking no precautions to exclude air. Warm water was used to melt the hydrogen donor and effect mixing of the reactants. The samples were placed upright in a temperature equilibrated Lundberg muffle furnace and heated at the indicated temperatures for the given times. The samples were then removed from the oven, cooled to room temperature and diluted with ca. 0.5 mL of dichloromethane. The samples were filtered through a plug of MgSO_4 and glass wool. An additional 0.5 mL of dichloromethane was used to wash the filter and, in catalytic reactions, the carbon black catalyst. An aliquot of the resulting solution was analyzed by gas chromatography.

RESULTS AND DISCUSSION

To facilitate the discussion of the results we identify in the structural formula of 4-(1-naphthylmethyl)biphenyl (I) different bonds that can be potentially cleaved, by the letters a through e, and identify in Table 1 the compounds that are formed after cleavage.



The conversion of I was studied under a variety of reaction conditions. The majority of the reactions were performed in the presence of 9,10-dihydro-phenanthrene (9,10-DHP) as hydrogen donor. Several experiments however, were performed in the absence of the hydrogen donor.

The overall conversion of I to products is given in Tables 2 and 3 for the reactions performed in the presence of 9,10-DHP under thermal and catalytic conditions at various temperatures and reaction times. As shown in Table 2, the thermal reaction is insignificant even at 400°C, (ca 3% conversion), and becomes important only at higher temperatures (18% at 419°C). Under the same reaction conditions, but with the addition of 5% Black Pearls 2000 (BP 2000) catalyst, the conversion at 400°C is ca 34%, and at 419°C it is increased to 63%. Using the data in Table 3 we have found that the cleavage of bond a follows reasonably well, first order reaction kinetics under both thermal and catalytic conditions.

Aside from increasing the overall rate of reaction of I, we found that this carbon black is an extremely selective catalyst for bond cleavage. Table 4 gives the product distribution obtained from I under thermal and catalytic conditions at 419°C. In the absence of the catalyst, bonds a and d are cleaved to almost the same extent, with nearly equimolar quantities of 4-methylbiphenyl (MeBz₂) and naphthyl tolyl methane (NTM) being produced. Bond b (1-methyl-

naphthalene and bibenzyl products) is cleaved only to a very limited extent. In the presence of the catalyst, however, a remarkable selectivity toward cleavage of bond a is observed as seen in the increased amount of MeBz₂ formed. In fact, cleavage of bond a is practically the only reaction promoted by this catalyst. This activity and selectivity were observed for all temperatures and catalyst concentrations studied.

Reaction rate constants and activation energies for thermal and catalytic reactions are given in Tables 5 and 6. The values for these parameters illustrate the dramatic effect of the added catalyst on the reaction of I in the presence of 9,10-DHP. One of the most important results is the large difference in the activation energies calculated for the thermal and catalytic reactions for the cleavage of bond a; E_a is ~60 kcal/mole for the thermal reaction (Table 5) and 17-25 kcal/mole for the catalytic reactions (Table 6). The variation of the activation energy with the quantity of catalyst (Table 6) is an indication that diffusion may play a role in the catalytic process (3).

When I is allowed to react in the absence of the hydrogen donor, the selectivity of the thermal reaction changes and cleavage of bond d is favored. The catalytic reaction, in the absence of 9,10-DHP, still shows the same remarkable selectivity toward bond a cleavage (Table 7). In the absence of hydrogen donor, however, compounds heavier than I are formed in all experiments, indicating that I is acting as a hydrogen source by dehydrogenation and condensation reactions. Besides these heavier compounds we also observed the formation of some methylidihydrophenanthrene, formed perhaps by cyclization of MeBz₂.

In order to put into perspective our findings regarding the high activity and exceptional selectivity of the BP 2000 catalyst in reactions with 4-(1-naphthylmethyl)bibenzyl, I, it is worth discussing the following points.

When the reactions of I, both with and without 9,10-DHP, are performed in the presence of a graphite carbon (Alfa) or of Illinois No. 6 coal, there is no increase in conversion of I above the thermal level nor is there any enhanced bond cleavage selectivity. Whether the behavior of BP 2000 is due to its physical structure or some other property is currently under investigation.

The BP 2000 catalyst appears to be specific for the cleavage of bonds between saturated carbons and polycyclic aromatic structures. This is illustrated by the reaction of diphenylmethane with BP 2000, both with and without 9,10-DHP. Even at 420°C, 1h, the methylene linkage in this compound remains intact.

Cleavage of bonds between methyl groups and polycyclic aromatic radicals in the presence of hydrogen donors has been explored extensively by McMillen, et al. (4). They have rationalized this reaction as a "solvent mediated hydrogenolysis", involving a H-transfer by a free radical mechanism. In this mechanism, a dihydroaromatic forms an ArH₂· free radical in a rate-determining step. The ArH₂· free radical then transfers a H-atom to the ipso position of the substituted polycyclic compound. The cyclohexadienyl-type free radical thus formed from the latter undergoes the aromatic carbon-methylene carbon bond scission. The above mechanism may be operating alongside other pathways, in the reaction of I in the presence of H-donors. Our findings for the reaction run in the presence of BP 2000, but in the absence of H-donor suggest however, that the radical-transfer sequence cannot be the prevailing mechanism for the cleavage of bond a in I under the catalytic conditions which we investigated.

Our work shows that it is possible to have high selectivity in breaking specific bonds under mild conditions if proper catalysts can be identified. Experiments are in progress toward the goal of understanding the mechanism of action of the BP 2000 catalyst. We are also investigating its use as a catalyst

for cleavage reactions in diquinolyl ethane and dehydroxylation reactions of some phenols.

CONCLUSIONS

Our study of the decomposition 4-(1-naphthylmethyl)bibenzyl as a model for reactivity of methylene and ethylene linkages during coal liquefaction showed that, in the presence of a hydrogen donor, the bond connecting 2 benzylic carbons and the bond between naphthyl and methylene units in naphthylphenyl methane, are broken with the same probability in a thermal reaction. We discovered that a high surface area carbon black (Cabot Corp., Black Pearls 2000) is a very active and selective catalyst for the cleavage of the naphthyl-methylene bond.



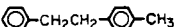
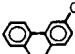
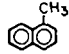
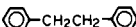
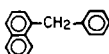
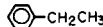
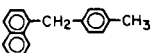
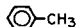
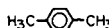
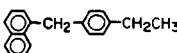

ACKNOWLEDGEMENTS

We would like to thank Prof. Paul Dowd and his group at the University of Pittsburgh for the synthesis and characterization of compound I, Louise Douglas for GC/MS work, and Prof. Dan Farcasiu for helpful discussions. This work was supported in part by an appointment to the Postgraduate Research Training Program under Contract No. DE-AC05-76OR00033 between the U.S. Department of Energy and Oak Ridge Associated Universities.

REFERENCES

1. Whitehurst, D.D.; Mitchell, T.O.; Farcasiu, M. "Coal Liquefaction The Chemistry and Technology of Thermal Processes" Academic Press: NY, 1980.
2. Kaminsky, M.; Yoon, K.J.; Geoffroy, G.L.; Vannice, M.A. J. Catal. 1985, 91, 338. Venter, J.J.; Vannice, M.A. J. Amer. Chem. Soc. 1989, 111, 2377.
3. Satterfield, C.N. "Mass Transfer in Heterogeneous Catalysis" MIT Press: Cambridge, MA, 1970.
4. McMillen, D.F.; Malhotra, R.; Chang, S.-J.; Ogier, S.; Nigenda, S.E.; Fleming, R.H. Fuel, 1987, 66, 1611. McMillen, D.F.; Malhotra, R.; Hum, G.P.; Chang, S.-J. Energy & Fuels, 1987, 1, 193.

TABLE 1.
IDENTIFICATION OF PRODUCTS RESULTING
FROM BOND CLEAVAGE OF
4-(1-NAPHTHYLMETHYL)BIBENZYL, I.


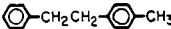
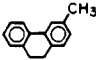
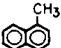
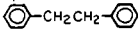
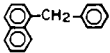
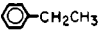
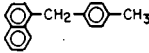
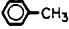

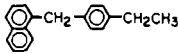

Bond Cleaved	Observed Products	Name	Symbol
a		Naphthalene	N
		Tetralin ¹	Te
		4-Methylbibenzyl	MeBz ₂
		3-Methyl-9, 10-dihydrophenanthrene ²	Me-9,10-DHP ²
b		1-Methylnaphthalene	MeN
		Bibenzyl	Bz ₂
c		1-(Naphthyl)phenyl methane	NPM
		Ethyl benzene	EtB
d		1-(Naphthyl)-4-tolyl methane	NTM
		Toluene	To
		p-Xylene ³	pX
e		1-(Naphthyl)-4(ethyl phenyl) methane	NEPM
		Benzene	B

1 From hydrogenation of N

2 From cyclization of MeBz₂

3 From further fragmentation of NTM

TABLE 1.
IDENTIFICATION OF PRODUCTS RESULTING
FROM BOND CLEAVAGE OF
4-(1-NAPHTHYLMETHYL)BIBENZYL, I.

<u>Bond Cleaved</u>	<u>Observed Products</u>	<u>Name</u>	<u>Symbol</u>
a		Naphthalene Tetralin ¹	N Te
		4-Methylbibenzyl	MeBz ₂
		3-Methyl-9, 10- dihydrophenanthrene ²	Me-9,10-DHP ²
b		1-Methylnaphthalene	MeN
		Bibenzyl	Bz ₂
c		1-(Naphthyl)phenyl methane	NPM
		Ethyl benzene	EtB
d		1-(Naphthyl)-4- tolyl methane	NTM
		Toluene	To
		p-Xylene ³	pX
e		1-(Naphthyl)-4 (ethyl phenyl) methane	NEPM
		Benzene	B

¹ From hydrogenation of N

² From cyclization of MeBz₂

³ From further fragmentation of NTM

Table 2. Influence of Temperature on Overall Conversion of I to Products at x% Carbon Black BP 2000 Catalyst.¹

Temperature °C	Conversion at x% Catalyst			
	0	2	5	10
320	0	0.8	---	3.9
360	0	4.6	15	23
375	0	9.1	16.2	27.0
400	3.0	17.6	33.6	43.6
408	7.3	---	49.8	---
419	17.8	42.7	63.0	77.0
429	28.7	53.8	78.9	87.2

¹Reaction conditions: 1h; wt ratio I:9,10-DPH 1:4; catalyst wt based on I.

Table 3. Influence of Reaction Time on Overall Conversion of I to Products at 421°C and x% Carbon Black BP 2000 Catalyst.¹

Reaction Time Minutes	Conversion at x% Catalyst		
	0	5	10
30	7.1	39.1	58
60	17.8	63	77
90	24.5	67	86.6

¹Reaction conditions: 1h; wt ratio I:9,10 DPH 1:4; catalyst wt based on I.

Table 4. Moles of Compounds¹ Formed/100 Moles I Consumed at x% Carbon Black BP 2000 Catalyst.²

Compound	Moles Compound Formed at x% Catalyst			
	0	2	5	10
To	52.1	10.1	4.9	2.5
pX	3.8	5.7	6.0	4.7
Te	14.1	21.3	24.8	25.8
N	22.4	64.4	68.4	64.6
MeN	3.6	4.3	4.3	3.9
Bz ₂	4.4	5.1	5.4	5.9
MeBz ₂	40.2	77.8	82.0	88.6
NTM	52.1	10.1	4.9	2.5

¹Refer to Table 1 for compound identification.

²Reaction conditions: 419°C; 1h; wt. ratio I:9,10-DPH 1:4; catalyst wt based on I.

Table 5. Reaction Rate Constants (k) and Activation Energies (E_a) for Thermal Reactions of Bonds a and d of I.¹

Temperature °C	k _a × 10 ⁻⁴ (min ⁻¹)	k _d × 10 ⁻⁴ (min ⁻¹)
400	~ 2.4	~ 2.7
408	5.2	6.1
419	12.5	16.3
429	18.3	26.7
E _a bond a (kcal/mol) ~ 60		E _a bond d (kcal/mol) ~ 70

¹Reaction conditions: 1h; wt. ratio I:9,10-DPH 1:4.

Table 6. Reaction Rate Constants (k) and Activation Energies (Ea) for Catalytic Reaction of Bond a of I at x% Carbon Black BP 2000 Catalyst.¹

Temperature °C	k x 10 ⁻⁴ (min ⁻¹) at x% Catalyst ²		
	2	5	10
360	7.9	27.1	43.6
400	26.3	60.9	86.8
408	----	92.2	----
419	47.7	100.2	149.4
429	48.2	116.2	146.6
Ea at x% catalyst (kcal/mol)	~25	~19	~17

¹Reaction conditions: 1h; wt. ratio I:9,10-DPH 1:4; catalyst wt based on I.

²Reported for catalytic contribution only. Thermal background has been subtracted.

Table 7. Moles of Compounds¹ Formed/100 Mol I Consumed in the Absence of 9,10-DPH Under Thermal and Catalytic Conditions.²

Compound	Moles Compound Formed at x% Catalyst ³	
	0 (7.5)	5 (25.3)
To	70.6	35.4
pX	0	4.3
N	4.8	52.4
MeN	3.7	7.2
Bz ₂	3.4	5.2
MeBz ₂	19.3	49.6
NPM	17.4	8.5
NTM	70.6	35.4

¹See Table 1 for compound identification.

²Reaction conditions: 408°C; 1h; catalyst wt based on I.

³Overall conversion of I at x% catalyst given in parentheses.

HYDROCRACKING WITH NEW SOLID ACID CATALYSTS: MODEL COMPOUNDS STUDIES.

Ramesh K. Sharma, John W. Diehl, and Edwin S. Olson

Energy and Environmental Research Center
University of North Dakota
Grand Forks, ND 58202

Two new solid acid catalysts have been prepared by supporting zinc chloride on silica gel and acid-exchanged montmorillonite. The acid properties of these catalysts were determined by Hammett indicator method which showed that highly Bronsted acidic sites were present. SEM/EDS studies indicated a uniform distribution of silicon, zinc, and chlorine in the silica gel-zinc chloride catalyst. The activities of these catalysts in the hydrocracking of bibenzyl, polybenzyl, alkylbenzenes, and other heteroatom substituted aromatics were investigated. Products from these reactions were analyzed by GC/FTIR/MS/AED and are consistent with an ionic or acid-catalyzed mechanism. High conversions to benzene and other small molecular weight products depend not only on the presence of strong acid sites but also on the ability of the catalyst to promote hydrogenation of complexed cationic intermediates, rather than condensation to oligomeric or polymeric (retrograde) materials. Our results with model compounds account for the effectiveness of these solid acid catalysts for conversion of coals to lower molecular weight materials.

Key words: Depolymerization, solid acid catalyst, hydrocracking

INTRODUCTION

New concepts are required in designing catalysts for coal liquefaction to produce distillate fuels with a low content of heteroatoms such as sulfur, oxygen, and nitrogen. In a two stage process, heteroatoms are removed by catalytic hydrotreatment of high molecular weight coal liquids produced in a preliminary low-severity process. The preparation and use of strong acid-catalysts and superacids are active areas of research for isomerization, cracking, hydrocracking, alkylation, acylation, methanol to gasoline, etc. (1). Because of the reported advantages of the solid acid catalysts (2), recent research has focused on the preparation and characterization (2-6) of stronger acid catalysts.

Although molten zinc chloride effectively depolymerizes coals (7,8), significant hydrodesulfurization of aryl sulfur compounds is not effected with this reagent (9). Other disadvantages of zinc chloride are its difficulty of recovery and corrosive nature. In a recent paper we reported a solid catalyst prepared by supporting zinc chloride on silica gel to be effective in hydrodesulfurization of diphenyl sulfide and dibenzothiophene(10). In this paper we report the preparation and characterization of solid acid catalyst prepared by supporting zinc chloride on acid-exchanged montmorillonite. The catalytic hydrotreatment of bibenzyl, polybenzyl, cumene, 1-phenyldecane, and n-hexadecane with silica gel and acid-exchanged montmorillonite supported zinc chloride, and acid-exchanged montmorillonite catalysts is being reported here.

EXPERIMENTAL

Reagents

Bibenzyl, cumene, 1-phenyldecane, n-hexadecane and zinc chloride were obtained from

Aldrich. Montmorillonite was obtained from Clay Spur, Wyoming and purified as reported (11).

Preparation of Polybenzyl:

Dichloromethane (200 ml) was placed in a three necked round bottomed flask (500 ml) fitted with three septa, one for the nitrogen inlet syringe needle, a second for the nitrogen outlet syringe needle (oil bubbler), and third for injecting the reactants. The flask was flushed with dry nitrogen, and 40 ml of stannic chloride was injected into the flask. Freshly distilled benzyl chloride (40 ml) was added to the flask with occasional stirring. After the addition was over, the reaction mixture was allowed to age at room temperature for four hours. At this stage the reaction mixture was quenched by slowly (dropwise) adding ice-cold methanol. When the reaction subsided, 200 ml more of ice-cold methanol was added. A yellow viscous solid was formed. The cloudy supernatant liquid was poured off, and the precipitate was washed several times with ice-cold methanol, dilute NaOH, deionized water, and methanol. The resulting solid was dissolved in a minimum amount of dichloromethane and freeze dried. The dried polymer was redissolved in a minimum amount of tetrahydrofuran by adding a large volume of methanol. The precipitate was filtered, washed with methanol and dried in vacuo.

Preparation of Catalysts:

Preparation of acid-exchanged clay (AM): Sodium-exchanged clay (5.0 g) was suspended in 200 ml of 0.1N HCl and stirred for three hours. The acid washed clay was separated by centrifugation, and washed with deionized water until free of chloride ions. The resulting clay was air dried. Final drying was accomplished by heating the clay at 250°C until constant weight was achieved.

Silica gel and acid-exchanged montmorillonite supported zinc chloride catalysts were prepared as described earlier (10). Total acidity and pKa's of the catalysts were determined by n-butylamine titrations using Hammett indicators (12).

Analytical procedures; Instrumentation:

Carbon, hydrogen, and nitrogen analyses were performed on Control Equipment Corporation Model 240XA Elemental Analyzer. The method of Vogel (13) was used for chlorine analysis. Proton and ¹³C NMR spectra were obtained in d₂-dichloromethane with TMS as standard on a Varian XL200 NMR spectrometer. Infrared spectra were recorded in KBr on either a Perkin Elmer Model 283 spectrophotometer or a Nicolet 205XB FTIR spectrometer equipped with a mercury cadmium telluride (MCTA) detector, and a Nicolet 1280 computer with a fast Fourier transform coprocessor.

Weight averaged molecular weight determination was performed in THF by gel phase chromatography (GPC, Waters Associates Liquid Chromatograph Model M6000) on a triple column (microstrogel) system calibrated with polystyrene and aromatic standards in the molecular weight range 34,500 to 202 and with UV detection.

Quantitative GC/FID analyses were performed with a Hewlett Packard 5880A gas chromatograph equipped with J&W 60 m x 0.25 mm (i.d.), 1.0 micron DB-1701 capillary column. n-Octadecane was the internal standard. Isotope dilution GC/MS was performed on a Finnigan 800 ITD ion trap detector with an HP 5890A gas chromatograph and a J&W 30 m x 0.32 mm (i.d.), 1.0 micron film of DB-5. Phenol, naphthalene, and tetralin were determined with the per-deuterated analogs as the respective internal standards. A 15 m x 0.25 mm (i.d.), 0.25 micron DB-5 film capillary column was used for the analysis of high boiling components.

Hydrocracking reactions:

In a typical run, 1.0 g of substrate and 0.5 g of the desired catalyst were placed in a tubing bomb (12 ml microreactor). The microreactor was evacuated, pressurized with 1000 psig of hydrogen, and placed in a rocking autoclave heated to 350°C. The heating continued for three hours. At the end of the reaction period, the microreactor was cooled to room temperature, degassed, and opened. The desired amount of internal standard was added to the product slurry, the product slurry was transferred into a centrifugation tube by washing with methylene chloride, and the solid catalyst was removed by centrifugation. The liquid sample was analyzed by gas chromatography/flame ionization detection (quantitative) and gas chromatography/Fourier transform infrared spectroscopy/mass spectrometry/atomic emission spectroscopy (14).

For the reaction of polybenzyl, the microreactor was attached to a series of three pre-weighed traps that were cooled in air, dry ice-acetone, and liquid nitrogen. The microreactor was slowly heated (3°C/min) to 250°C and held at this temperature until distillation stopped. The distillate was weighed, and dissolved in 10 ml methylene chloride. This solution was mixed with appropriate internal standards and analyzed by GC/FID, isotope dilution GC/MS, and GC/FTIR/MS/AED. The undistilled product was extracted with THF and separated into THF-soluble and insoluble fractions. Both these fractions were vacuum dried, weighed, and analyzed by FTIR, elemental analysis, and m.w. determinations.

Results and Discussion:

Elemental analysis of zinc chloride supported on silica gel (SZC) and acid-exchanged montmorillonite (AMZC) suggests a high loading of zinc chloride on the support surface. Most of the chlorine is present as zinc chloride (Ca. 98%), and only a small amount of chlorine (<3%) is present as M-O-Zn-Cl. SEM/EDS studies indicated a uniform distribution of silicon, zinc, and chlorine in the silica gel-supported zinc chloride catalyst (10). In this paper we prepared another catalyst by supporting zinc chloride on acid-exchanged montmorillonite. The pKa's and total acidity of silica gel-zinc chloride, acid-exchanged montmorillonite-zinc chloride, and acid-exchanged montmorillonite were determined by n-butyl amine titrations using Hammett indicators, and results are presented in (Tables 1 and 2).

TABLE 1
ACID STRENGTH ON CATALYST SURFACE

Catalyst	pKa						
	-5.6	-8.2	-11.30	-11.99	-12.70	-13.75	-14.56
SZC	+	+	+	+	-	-	-
AM	+	-	-	-	-	-	-
AMZC-B	+	-	-	-	-	-	-

- + Color of the conjugate acid of a basic indicator appeared on the surface.
- The above color did not change.

TABLE 2
TOTAL ACIDITY BY AMINE TITRATION

Indicator	pKa	Amount of Acid (mmole/g)		
		SZC	AM	AMZC-B
m-Nitrotoluene	-11.99	0.71		
p-Nitrotoluene	-11.30	0.97		
Benzalacetophenone	-5.6	1.96	1.28	1.55

The total number of moles adsorbed using amine titration was based on the benzalacetophenone as an indicator (all acid sites with strength up to $pK_a = -5.6$ were determined). Due to the brown color of acid-exchanged montmorillonite-zinc chloride catalyst, the detection of color change was difficult. Therefore, this catalyst was mixed with silica gel-zinc chloride with a known acidity prior to titration with n-butyl amine. These titrations indicate that silica gel-zinc chloride catalyst has the greatest number of acid sites, and acid-exchanged montmorillonite the fewest. Comparison of the total amount of acidity for silica gel-zinc chloride catalyst using benzalacetophenone ($pK_a = -5.6$), p-nitrotoluene ($pK_a = -11.3$), and m-nitrotoluene ($pK_a = 11.99$) indicated a decrease in the total acidity as the pK_a of the of the indicator changed from -5.6 to -11.3.

The acid strength for the three catalysts, as determined by the amine titration, is provided in Table 1. For the silica gel zinc chloride the acid strength H_0 lies between -5.6 and -12.7 ($-5.6 < pK_a < -12.70$). Acid-exchanged montmorillonite, and acid-exchanged montmorillonite-zinc chloride have acid strength $H_0 \leq 5.6$. Comparing the results of the acidity measurements of the three catalysts it appears that silica gel-zinc chloride is most acidic among the catalysts investigated.

Catalytic hydrocracking of model compounds:

In order to understand the nature and extent of catalytic activity of supported zinc chloride, reactions of bibenzyl, cumene, 1-phenyldecane, and n-hexadecane were investigated. All reactions were carried out with or without solvent in the presence of 1000 psig molecular hydrogen at 350°C for three hours. The catalyst-to-substrate ratio was 0.5. Percent conversion, which is a measure of the aryl-carbon bond cleavage, was calculated on the basis of the starting material reacted. The results are given in Table 3 as product yields (mmoles) and percentage conversion of the substrate to the products.

TABLE 3

CATALYTIC HYDROCRACKING OF MODEL COMPOUNDS
(1000 psig H₂ pressure, 350°C, 3 hrs, catalyst wt/substrate wt = 0.5)

Catalyst (g)	Substrate (mmoles)	Solvent (mmoles)	Conv. (%)	Major Product (mmoles)
none	BB (5.49)	none	1	toluene (trace)
SZC (0.50)	BB (5.49)	none	85	benzene (3.35) ethylbenzene (3.26)
*SZC (0.50)	BB (5.49)	none	70	benzene (3.14) ethylbenzene (3.03)
SZC (0.50)	BB (5.49)	p-Cresol (18.52)	37	phenol (2.27)
SZC (0.50)	p-Cresol (9.44)	none	80	phenol (2.04)
AM (0.50)	BB (5.49)	none	75	benzene (4.89)
AMZC (0.50)	BB (5.49)	none	66	benzene (3.96)
SZC (0.50)	Cumene (8.33)	none	99	benzene (1.84)
SZC (0.50)	1-Phenyldecane (4.59)	none	40	benzene (0.65) C ₁ -C ₆ benzenes
SZC (0.50)	n-Hexadecane (4.42)	none	20	C ₃ -C ₆ alkanes

• = aged catalyst

BB = bibenzyl

A blank reaction of bibenzyl (without catalyst) gave almost complete recovery of the starting material, and only a trace amount of toluene was detected. No benzene or ethylbenzene were observed in the products. However, when bibenzyl was reacted with zinc chloride supported on silica gel, 85.5% of bibenzyl was converted into smaller molecules. The major products from this reaction were benzene, toluene, and ethylbenzene. Small amounts of propylbenzene, butylbenzene, tetralin, benzylethylbenzene, benzylpropylbenzene, etc. were also formed. No chlorine from the catalyst was found to be incorporated into the organic products. The catalyst was recovered in almost quantitative amounts, and the chlorine contents were the same as in the starting catalyst. The amount of coke or polymeric material in the recovered catalyst that could have been formed due to acid-catalyzed retrograde condensation reaction was negligible, and no corrosive melt was formed. In a reaction with aged catalyst, lower conversion (70%) of bibenzyl was observed. Aging, or perhaps

exposure of the catalyst to atmospheric conditions may have changed the nature of the acidity of the catalyst (10).

Although this catalyst gave high conversion in the absence of solvent, a suitable solvent may be necessary for this catalyst to be useful for the coal liquefaction. Reaction of bibenzyl in p-cresol (solvent) was investigated. In contrast to the neat reaction, the conversion was low (37%) in this solvent. In addition, only 39% p-cresol was recovered at the end of the reaction. Bibenzyl gave the same major and minor products as in the reaction without solvent, but in much smaller amounts than expected. Bibenzyl substituted cresol, tetralin, naphthalene, anthracene, naphthol, and mono, and dimethylbibenzyl were some of the products. In order to understand the role of the solvent in the cleavage reactions, p-cresol was reacted with this catalyst and hydrogen under the same reaction conditions as those used for bibenzyl. Reaction of the solvent alone resulted in 80.4% conversion of cresol to other products. Only 27% of the expected phenol was formed. Dimethylphenols and phenoxyphenol were some of the other products of this reaction. The high reactivity of cresol eliminates it from consideration as a solvent. Under strongly acidic conditions, it apparently condenses extensively to high molecular weight products. Solutes also would become involved in these condensations.

In order to further demonstrate that the Bronsted and/or Lewis acidity was responsible for the reductive cleavages of aryl-methylene bonds, reactions of bibenzyl were also carried out with acid-exchanged montmorillonite and acid-exchanged montmorillonite supported zinc chloride. These reactions gave 75 and 66% conversions for acid-exchanged montmorillonite and acid-exchanged montmorillonite supported zinc chloride, respectively. A majority of the product was benzene, and small amounts of toluene, o-xylene, and ethylbenzene were also formed. In addition, almost 40% of the product was polymeric material, mainly polybenzyls. The origin of this polymeric material may have been acid-catalyzed polymerization of the benzyl species formed during initial stages of the reaction. Because of formation of the condensation products from the hydrotreating of bibenzyl with these catalysts, their effectiveness in hydrotreating coal liquids might be questioned. With regard to avoiding extensive condensation reactions, the zinc chloride supported on silica gel is most effective. Nevertheless, the zinc chloride supported on acid-exchanged montmorillonite gave respectable conversions in the hydrotreating of low severity liquefaction products from Wyodak subbituminous coal (15).

Although the conversions were high, the product yields are suggestive of the fact that only one aryl-methylene bond is cleaved under the reaction conditions employed. In order to further understand the mechanism of this reaction, iso-propylbenzene (cumene) was reacted with zinc chloride supported silica gel. This reaction gave almost complete conversion of the iso-propylbenzene, and benzene was the major product. The reaction of 1-phenyldecane with this catalyst gave 40.3% conversion. A large number of products were formed from this reaction. Major products were benzene, toluene, ethylbenzene, propylbenzene, butylbenzene, pentylbenzene and hexylbenzene, indane, etc.

Examination of the products obtained from the reaction of n-hexadecane with zinc chloride supported silica gel indicated 20% cracking to smaller molecules. Major products of this reaction being propane, butane, pentane, and hexane etc. The low conversion suggests that this catalyst may be useful for cleaving bonds attached to aromatic rings in coal macromolecules without unwanted cracking of alkanes to gases. No cracking of alkanes was observed when they were used as solvents for the model compound reactions.

In silica gel supported zinc chloride catalyst, highly acidic Bronsted sites are available due to the silica hydroxyls associated with zinc chloride. Protonation of the ipso position of the ring will give the arenium ion intermediate, which can

undergo aryl-methylene bond cleavage. The presence of benzylethylbenzene, benzylpropylbenzene, etc. in the hydrotreating products is indicative of carbonium ion intermediates in the reaction of bibenzyl. Formation of a "surfacebound" carbonium ion is hypothesized to explain the lack of extensive condensation that might occur if free carbonium ions were formed. Since the reaction rate is much higher with secondary alkyl groups (cumene reaction), it is clear that the reaction proceeds rapidly whenever the cationic leaving group can be stabilized by α - or β -phenyl groups or alkyl groups, and more slowly or with extensive rearrangement when the leaving group is primary (1-phenyldecane reaction). It is clear that the acid catalyst is effective in cleaving aryl-methylene bonds at relatively lower temperature and without chlorine substitution or extensive condensation of carbonium ion intermediates.

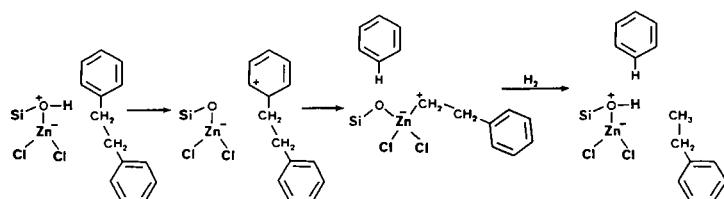


Figure 1. ACID-CATALYZED MECHANISM

Research is in progress to characterize the spent catalyst and to test the catalytic activity of the spent catalysts at higher temperatures.

Catalytic hydrocracking of model polymer:

Model coal polymers with well defined structures, thermally more stable than polystyrene or polybenzyl ethers, are needed for testing of hydrotreating reactions in order to understand the coal liquefaction. The synthesis of a model coal polymer, which meets the criteria of being highly branched, highly soluble, and thermally stable, has been accomplished. It was not clear from the literature that this is a bulky (branched) polymer; however, the thermal stability is good because of the methylene bridges between the benzene rings.

The infrared of the polymer showed a weak absorption in the 800-850 cm^{-1} range, corresponding to two adjacent hydrogens on an aromatic ring. This indicates that the para substituted benzene components of the polymer structure are relatively minor, probably less than 10%. Because of the intense absorption at 740 to 760 cm^{-1} , corresponding to monosubstituted benzenes, the structure must be highly branched containing many (90%) benzyl groups attached to the backbone system. A weak absorption at 900 cm^{-1} , corresponding to single hydrogens on an aromatic ring, was also present in the spectrum. This absorption is usually weak, thus there are still some unsubstituted aromatic positions in the backbone system. The highly branched structure explains the high solubility of the polymer in organic solvents. NMR evidence shows that there are anthracene groups, but no chloromethyl groups.

The anthracene is undoubtedly formed by oxidation of dihydroanthracene by the stannic chloride. Although the formation of dihydroanthracene terminates the chain in terms of obliterating the electrophilic chloroethyl groups, the reaction of additional benzyl groups on the polymer can occur at any point. Thus, the

anthracene may not necessarily be on the end of the chain. Calculation of a molecular weight, based on the 1 to 23 ratio of anthracene to benzyl, gives a value of 2250 per anthracene unit. The weight average molecular weight was found from the GPC data to be 1300 daltons. The presence of anthracene units in the polymer will, however, delay the elution of the polymer substantially and cause a severe error in the GPC determination, which is based on the calibration with polystyrene.

The hydrotreating of polybenzyl (C, 92.96; H, 6.98; H/C ratio, 0.9) with zinc chloride supported on silica gel and 1000 psig hydrogen at 350°C for 3 hours gave 61% distillate. The distillate was found to consist of 95% benzene, toluene, oxylene in approximately equimolar amounts. Small amounts of cyclohexane methylcyclohexane, C₃ and C₄ benzenes, naphthalene, indane, tetralin, methylnaphthalenes, and anthracenes were also present in the distillate.

Mass balance and infrared analysis of the THF-soluble fraction indicated a small amount of polymeric material (6.9%) present. THF-solubles (Vacuum bottoms, C, 89.5; H, 6.21; H/C ratio, 0.83) were 32.9% of the starting polymer. Detailed characterization of the THF-soluble fraction is in progress.

This experiment demonstrates that the silica gel-zinc chloride catalyst is effective in depolymerization of highly branched alkylbenzene polymers without extensive condensation to insoluble chars.

ACKNOWLEDGEMENT

This research was supported by Contract No. DOE-FC2186-MC10637 from the U.S. Department of Energy. References herein to any specific commercial product by trade name or manufacturer does not necessarily constitute or imply its endorsement, recommendation, or favoring by the United States Government or any agency thereof. The assistance of Jonathan Kautz is greatly appreciated.

REFERENCES

1. K. Tanabe, In *Heterogeneous Catalysis; Catalysis by Novel Solid Strong Acids and and Superacids*; B.L. Shapiro, Ed., Texas A&M University Press, College Station, TX (1984) 71-94.
2. J.C. Vedrine, A. Auroux, V. Bolix, P. Dejaifve, C. Naccache, P. Wierzchowski, E.G. Derovane, J.B. Nagy, J. Gilson, J.H.C. Van Hooff, J.P. Van Den Berg, and J.J. Wolthiozen, *Catalysis*, 59 1979 48-162.
3. H. Pines, *The Chemistry of Catalytic Hydrocarbon Conversion*, Academic Press, New York/London, (1981) 100-122.
4. G.A. Olah, G.K. Surya Prakash, and J. Sommer, *J. Superacids*. Wiley, New York, (1985) 53.
5. R.S. Drago, E.E. Getty, US Patent 4 719 190, January 12, 1988.
6. R.S. Drago and E.E. Getty, *J. Am. Chem. Soc.* 110 1988 3311-3312.
7. D.P. Mobley and A.T. Bell, *Fuel*, 59 1980 507-510
8. C.W. Zielke, R.T. Struck, J.M. Evans, C.P. Costanza and E. Gorin, *Ind. Eng. Chem. Proc. Des. Dev.*, 5 1966 158-164.
9. R.T. Struck and C.W. Zielke, *Fuel*, 60 1981 795-800.

10. R.K. Sharma, J.W. Diehl, and E. S. Olson, 3rd Int. Conf. on Proc. and Utilz. of High Sulfur Coals, Ames, Iowa, Nov. 14-16, 1989.
11. T.J. Pinnavaia, Science, 220 1983 365-371 and references therein.
12. K. Tanabe, Solid Acids and Bases, their catalytic properties, Academic Press, New York/London, (1970) 528.
13. A. Vogel, Textbook of Quantitative Inorganic Analysis, 4th edn., Longman Sci. and Tech. Group, Essex, Eng., (1978) 434.
14. E.S. Olson, and J.W. Diehl, Anal. Chem., 1987 443-448
15. E.S. Olson, J.W. Diehl, and R.K. Sharma, ACS Div. of Fuel Chem., Boston, MA, April, 1990 (communicated).

USE OF MODEL COMPOUNDS IN COAL STRUCTURE AND REACTIVITY STUDIES

Randall E. Winans, Ryoichi Hayatsu, Thomas G. Squires†,
Kathleen A. Carrado, and Robert E. Botto

Chemistry Division, Argonne National Laboratory, Argonne, IL 60439, and

†Associated Western Universities, Inc., Salt Lake City, UT 84124

INTRODUCTION

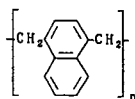
The interpretation of data from chemical and thermal reactions of coals is often facilitated and can be strengthened by investigating analogous reactions in appropriate model systems. While coal models have ranged from small molecules to polymers to synthetically coalified biomolecules and biomacromolecules, it appears that there are dangers in extrapolating the behavior of small, soluble molecules to that of solid coal. We have found that polymers and synthetic coals are much more appropriate models for coal behavior. In the present report, pyrolysis data from the latter models and coals will be compared and contrasted.

EXPERIMENTAL

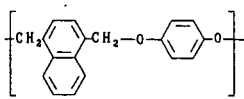
The compositions of the Argonne Premium coals and polymers used in this study are given in Table 1. The preparations of the coal samples¹ and of the two polymers² have been described.

TABLE 1. Elemental Analyses for the Argonne Premium Coal Samples.

Sample	Name	%C(maf)	Per 100 Carbons			
			H	N	S	O
8	Beulah-Zap Lignite	72.9	80	1.4	0.4	20.9
2	Wyodak-Anderson SubB	75.0	86	1.3	0.2	18.0
3	Illinois Herrin hvCB	77.7	77	1.5	1.2	13.0
6	Blind Canyon hvBB	80.7	86	1.7	0.2	10.8
7	Lewiston-Stockton hvAB	82.6	76	1.6	0.3	8.9
4	Pittsburgh hvAB	83.2	77	1.7	0.4	8.0
1	Upper Freeport mvB	85.5	66	1.5	0.3	6.6
5	Pocahontas lvB	91.0	59	1.3	0.2	2.0
	Polymer I	92.6	87	-	-	-
	Polymer II	79.6	84	-	-	11.0



I



II

Scheme 1.

GCMS and PYMS data were obtained on a Kratos MS-25 mass spectrometer. A 60 m x 0.25 mm DB-1701 fused silica column was used in GCMS analysis. The details of the PyMS experiment have been reported.³ The samples were all heated at 50°/min or at 75°/min on a platinum screen and the instrument was operated in the precise mass measurement mode.

For the very high resolution experiments, the samples were inserted into an all glass heated inlet system (300° C) and leaked into the source of a Kratos MS-50 ultra high resolution mass spectrometer.⁴ A dynamic resolution of 80,000 was obtained for the low voltage (11 eV) electron impact LVHRMS experiment with a scan rate of 1000 seconds/decade. The 70 eV EI spectra were obtained with 50,000 dynamic resolution with a scan rate of 100 seconds/decade. Both spectrometers were operated with a Kratos DS 90 data system. Data was transferred to a Micro Vax II for final analysis. The data are sorted by both heteroatom content and by hydrogen deficiency (HD). The term HD corresponds to number of rings plus number of unsaturations ($HD = -2Z$).

Synthetic Polymer Models

In the present investigation, we have examined the PyMS behavior of two synthetic polymers containing linkages presumed to exist in coals, an ethylene-linked naphthalene (I) and a hydroquinone-linked naphthalene (II). Our initial studies on the PyMS, oxidation, and liquefaction behavior of these polymers have been reported.² Solomon and coworkers have examined the pyrolysis products of similar polymers using FIMS.⁵ The PyMS techniques used in the present study have the distinct advantage of detecting and analyzing the pyrolysis products in the time-resolved mode, i.e. as soon as they are released to the vapor phase. From Figure 1, it is clear that polymer I is much less reactive than II. The pyrograms of I look much like those produced in the PyMS of inertinite macerals, with no major peak until the temperature reaches approximately 540°C. In contrast, the major devolatilization of polymer II occurs at a much lower temperature (310°C).

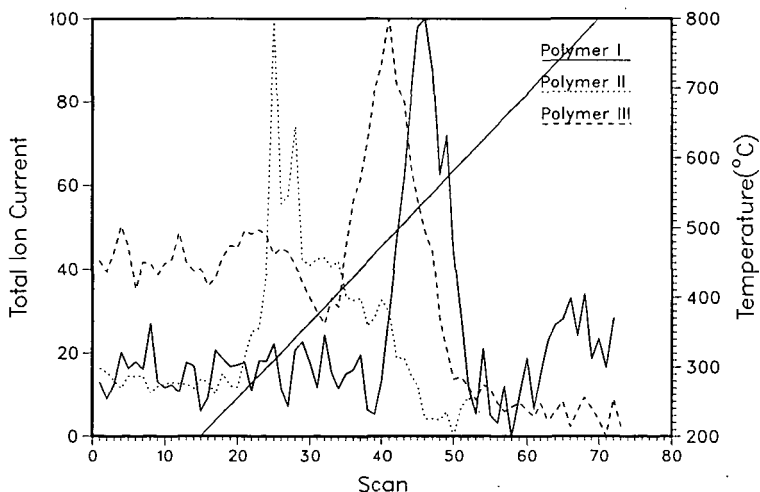
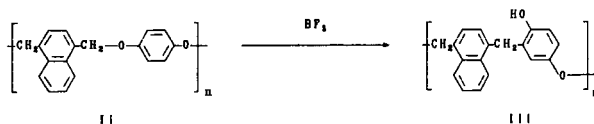


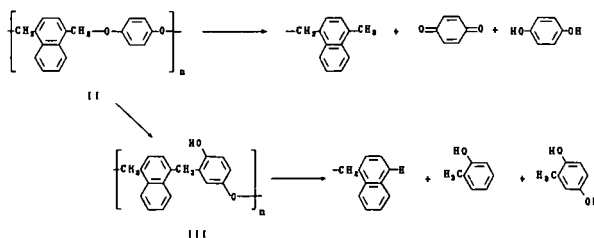
Figure 1. Total ion current pyrograms of the synthetic polymers heated beginning with scan 15 at 75° C/min from 200° to 800° in high resolution mode.

We have previously reported that attempts to unlink polymer II under mild acid conditions afforded only trace amounts of solubilized oligomeric product and almost quantitative rearrangement to a methylene linked polymer (III) as shown in Scheme 2.⁵ Both chemically and pyrolytically, the rearranged polymer, III, is much less reactive than the original oxymethylene-linked polymer, II. Pyrolysis of the rearranged polymer affords a major devolatilization peak at 480°C, 170°C higher than that of the original (Figure 1).



Scheme 2.

In addition, we have found the following convincing evidence that pyrolysis of the unrearranged oxymethylene-linked polymer II involves, as one of the reaction pathways, an analogous rearrangement to a methylene-linked polymer. In the PyMS of polymer II, a fragment with $M/Z=108$ can be due to quinone, a cresol, or a hydrocarbon. High resolution mass spectrometry makes it possible to differentiate among these species; and the results of using this technique in our PyMS experiments with polymer II are shown in Figure 2. At temperatures below 300°C, quinone but no cresols is detected while above 350°C, the reverse is observed. A very simple and reasonable explanation of these results is shown in Scheme 3.



Scheme 3.

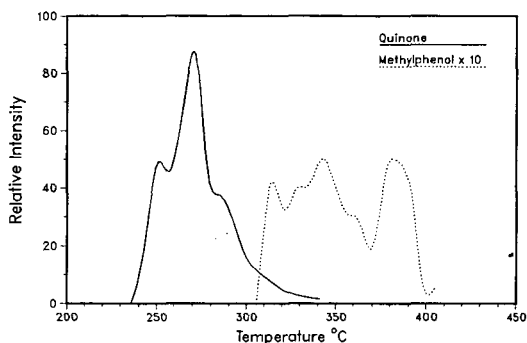


Figure 2. Selected ion chromatogram for quinone and methylphenol fragments from PyMS of Polymer II.

The time resolved high resolution MS data makes it possible to differentiate between these two different pyrolysis products even though they have the same nominal mass.

In light of these results from the model polymer, the data from PyMS of some of the Argonne Premium Coal Samples were examined for alkylated phenols and quinones. For the subbituminous coal (APCS #2) peaks which could be assigned quinone structures were observed at the lower temperatures. In Figure 3, the evolution of selected peaks are shown as a function of temperature. There is no evidence for quinones at the higher temperatures while alkylphenols are still observed. Higher rank coals such as the Illinois No. 6 (APCS #3) yielded only trace amounts of peaks corresponding to quinones while none were observed for coals with greater than 80% carbon, however, alkylphenols are observed.

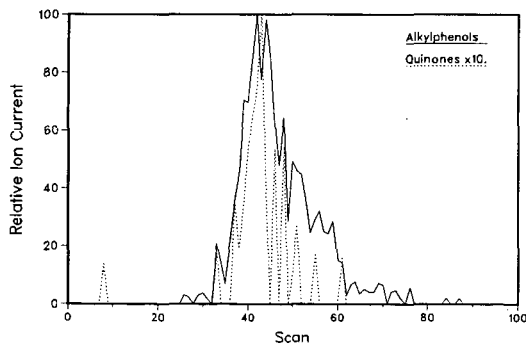
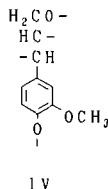


Figure 3. Selected ion pyrograms for the subbituminous coal (APCS #2).

Synthetic Coal Models

Lignins are thought to be the major precursors of vitrinite macerals. Synthetic vitrinites have been prepared heating the lignin with promotion by clays.⁷ Softwood lignins are made up mostly from the coniferyl alcohol monomers (IV). Some of the initial reactions are the loss of methyl and methoxyl with re-alkylation of the benzene ring. Also, studies of sediments confirm that these types of transformations occur.⁸



Model compounds of the softwood lignin structure were reacted under simulated coalification conditions in order to elucidate the clay-organic reactions responsible for bond cleavage and rearrangement processes in these systems. Of specific interest was the reactivity of anisole (phenyl methyl ether) groups in these model compounds, which include *m*-methyl anisole (mMA), guaiacol, 4-hydroxy-3-methoxy toluene and 4-phenoxy-3-methoxy toluene. Pillared clays (PILCs) were chosen as the catalysts because they are an order of magnitude more active than untreated clays under these specific conditions. PILCs are smectite clays with permanent intracrystalline porosity made by metal oxide molecular props, usually alumina, that hold the clay layers apart.

The predominant reaction observed is O-methyl bond cleavage of anisoles to lead to phenolic functionality. Transalkylation and dealkylation reactions are also observed by GCMS and solid-state ¹³C NMR techniques. In addition, isotopically labeled ¹³C anisoles were synthesized and reacted with clays. Mass spectra of volatile products reveal the presence of ¹³CH₃OH and large amounts of (¹³CH₂)₂O due to further dehydration of methanol over the clay surface.

Table 2 gives the distribution of solvent-extractable products obtained from mMA catalysis as determined by GCMS. The amount of mMA decreases as it is reacted to *m*-cresol and alkylated cresols (major products), and alkylated anisoles (minor products). The amount of dialkylated products begins to decline after a certain amount of reaction time, as they are further cracked to simpler products.

TABLE 2. Distribution (mole %) of soluble products obtained from the reaction of *m*-methyl anisole with pillared bentonite clay at 150° C.

Product	Time (hours)			
	0	22	49	72
mMA	100	69.2	9.4	4.9
Me-mMA	0	3.3	9.8	10.1
Me ₂ -mMA	0	0	1.8	1.0
<i>m</i> -cresol	0	27.7	33.2	34.8
Me-cresol	0	0	24.5	41.4
Me ₂ -cresol	0	0	21.3	7.8

mMA = *m*-methyl anisole

Me = methyl

These results give an indication of the types of reactions that occur under simulated coalification conditions. These necessarily involve heterogeneous interactions with a solid acid catalyst and reactions that are typically catalyzed by protons.

From the model studies one would predict that the number of benzene rings with two oxygen substituents would decrease with increasing rank. Also, the overall phenolic content should decrease with rank. PyHRMS data have been obtained for the eight Premium Coal Samples. An estimate of yields of phenols from the high vacuum pyrolysis is shown in Figure 4. The trends observed are as expected except for the Utah Blind Canyon Coal (APCS #6). This coal is rich in liptinites which would mean that the products would be dominated by the high yield hydrocarbons from the liptinites. Overall, the species with two oxygens decrease rapidly after about 78% carbon content. The Illinois No. 6 coal may be a little unusual since it has a fairly high oxygen content for a high volatile bituminous coal. There appears to be a significant amount of lignin character left in the lignite. This conclusion is supported by oxidative degradation data and by characterization of extracts from lignite.

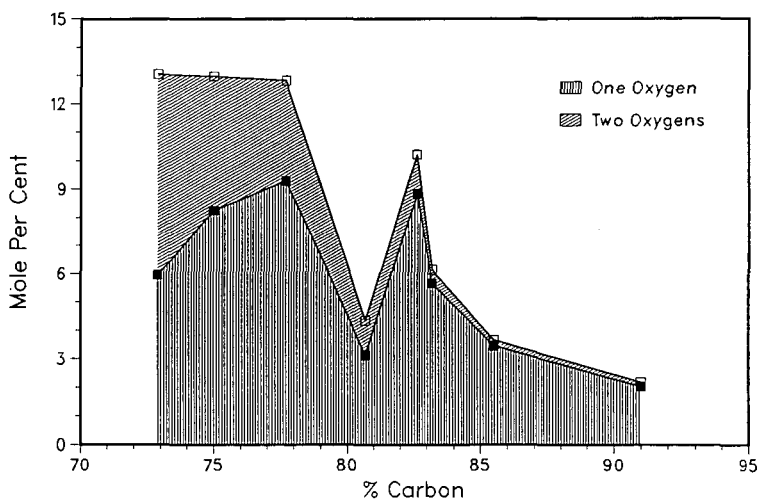


Figure 4. Phenols from PyHRMS of the Premium Coals presented as a stacked plot.

CONCLUSIONS

It would be very difficult to say anything about chemical structures in coals without results from model systems. Many times the systems were not studied as a model for coals, but the results can still be used to interpret the coal data when similar methods are used. Macromolecular models can be quite realistic and some of the examples described in this paper show how they can be used to better understand the coal results. However, one must be careful that the model results are not over-interpreted much like the problem that has occurred with drawing or modeling of "average structures."

ACKNOWLEDGMENTS

This work was performed under the auspices of the Office of Basic Energy Sciences, Division of Chemical Sciences, U.S. Department of Energy, under contract number W-31-109-ENG-38.

REFERENCES

1. Vorres, K.S.; Janikowski, S.K. *Preprints, Div. Fuel Chem., ACS* **1987**, *32(1)*, 492.
2. Squires, T.G.; Smith, B.F.; Winans, R.E.; Scott, R.G.; Hayatsu, R. *Proceedings International Conference on Coal Science* **1983**, p. 292.
3. Winans, R.E.; Hayatsu, R.; Scott, R.G.; McBeth, R.L. In *Chemistry and Characterization of Coal Macerals*; Winans, R.E.; Crelling, J.C., Eds.; ACS Symposium Series No. 252, ACS:Washington, D.C. **1984**; p. 137.
4. Winans, R.E.; McBeth, R.L.; Neill, P.H. *Preprints, Div. Fuel Chem., ACS* **1988**, *33(3)*, 85.
5. Squire, K.R.; Solomon, P.R.; Caranzelo, R.M.; DiTaranto, M.B. *Fuel* **1986**, *65*, 833.
6. Smith, B.F.; Venier, C.G.; Squires, T.G. *Preprints, Div. Fuel Chem., ACS* **1984**, *29(5)*, 15.
7. Hayatsu, R.; McBeth, R.L.; Scott, R.G.; Botto, R.E.; Winans, R.E. *Org. Geochem.* **1984**, *6*, 463.
8. Hatcher, P.G.; Lerch, H.E. *Preprints, Div. Fuel Chem., ACS* **1989**, *34(3)*, 617.

SYNTHESIS AND CONVERSION STUDIES OF POLYMERIC MODELS FOR LOW-RANK COALS

Donald F. McMillen and Ripudaman Malhotra

Chemical Kinetics Department, Chemistry Laboratory
SRI International, Menlo Park California, 94025-3493

and Michael A. Serio

Advanced Fuel Research
East Hartford, Connecticut 06108

KEYWORDS: Coal Models, Poly(eugenol), FIMS, Liquefaction, Pyrolysis

INTRODUCTION

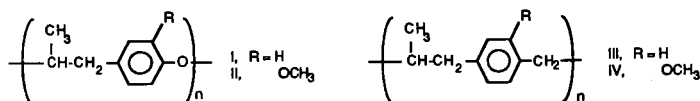
Efforts to understand the key chemical reactions responsible for coal conversion have been severely hindered over the years by the necessity of having to infer a complex sequence of chemical reactions for a substrate, coal, whose critical linkages are basically unknown. To aid in the effort, many workers have studied the reactions of coal "models" under various conversion conditions. However, this already imperfect solution has itself been limited by the inappropriateness of many of the models, and by the widespread misconception that the spontaneous thermal scission of inherently weak linkages in the coal structures is solely responsible for the fragmentation of the coal matrix. In fact, the combination of these two factors has compounded the situation: the perception of control by homolysis of weak linkages has led to a disproportionate focus on weakly bonded models such as bibenzyl, benzylphenyl ether, and related structures. This paper reports the initial results of an effort to use model structures that (1) have inter-cluster linkages that are perhaps more representative of those in coals, and (2) are incorporated into polymeric networks in order that mass transport and other effects that can be important in heterogeneous systems might be more appropriately mimicked.

The basic linkage chosen for the present study is the oxy-ethylene linkage of phenyl phenethyl ether. Although phenyl phenethyl ether and related structures have been previously studied as coal models (1-4), they have not received the attention commensurate with their recognized abundance in lignins. No studies, to our knowledge, have been reported for specially synthesized and characterized polymers containing this linkage. As it happens, the weakest bond in phenyl phenethyl ether, the phenoxy-carbon bond, is about equal in strength to the central bond in bibenzyl (5,6). At ~ 61 kcal/mol, the bibenzyl bond undergoes homolysis at 400°C with a half life of ~ 25 hours, but as has been well-demonstrated in studies of several three-atom-linked di-aryls (1-4), homolysis typically serves only as the initiation process for their decomposition. In the case of phenyl phenethyl ether itself, the very facile β -scission of the benzylic radical formed by H-abstraction results in an observed half-life (at 400°C) that is at least 10 times shorter than that for the homolysis (2). Clearly, either coals do not have very many such linkages, or some other factor (viz., retrograde reaction) counteracts the demonstrated reactivity of the $-\text{O}-\text{C}-\text{C}-$ linkage. Interestingly, low-rank coals have for a long time been known to be more reactive than bituminous coals, but they give lower liquefaction conversions. Therefore, it seems likely that a crosslinked or intertwined polymeric network, or the presence of additional functional groups (i.e., $-\text{OH}$, $-\text{OMe}$, or $-\text{COOH}$) result in a proclivity for retrograde reactions that makes coals with very labile linkages unusually hard to convert. To better understand those retrograde processes and the approaches that might be used to limit them, we have embarked on a program to synthesize, characterize, and study the conversion of the polymeric, three-atom-bridged models described below.

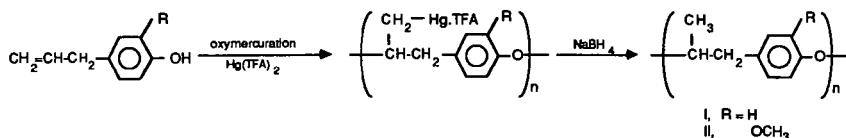
RESULTS

Polymer Synthesis

We prepared two three-atom-bridged polymers of the -O-C-C- type, and for a baseline comparison, the corresponding -C-C-C- type polymers. This paper focuses on the synthesis, characterization, and initial conversion studies of two variations of the -O-C-C- linked polymers.

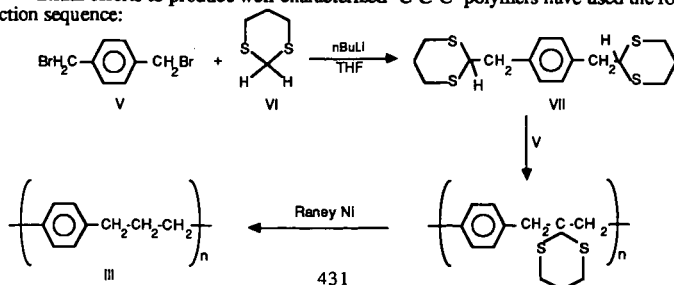


Polymers containing the -O-C-C- linkage between single phenyl rings have been prepared by the oxymercuration of eugenol (R = OCH₃) and 4-allylphenol (R = H). Eugenol was obtained from Aldrich Chemical, Inc. 4-Allylphenol was obtained by custom synthesis from Saber Laboratories (Morton Grove, Illinois). The polymerization was conducted at 80°C in nitromethane solvent using dry Hg(CF₃CO₂)₂ as a catalyst. The low nucleophilicity of the trifluoroacetate (TFA) allows for attack on the mercurated complex by the phenolic oxygen resulting in polymerization of the substrate. Mercury was removed from the initial polymerization product using sodium borohydride.



The polymers were characterized using elemental analysis, GPC, NMR, and field ionization mass spectrometry (FIMS). GPC shows that the poly(eugenol) sample discussed here has a broad distribution of molecular weights (1x10⁴ to 2x10⁶; M_n ~2x10⁵). The poly(p-allylphenol) sample, on the other hand, has a narrow MW range with a M_n ~5x10⁶. Light scattering experiments confirmed the very high molecular weights of these polymers. The polymers are insoluble in most common solvents and only sparingly soluble in cold DMF. However, they have high solubility in hot DMF. ¹H NMR peak area ratios were generally consistent with the expected ratios, but were not highly precise, owing to limited solubility in the cold DMF as well as interference from water and traces of protonated solvent in the deuterated DMF. ¹³C CPMAS NMR of the solid samples is also consistent with the expected structure, however, reliable quantitative information on the relative amounts of alkyl and aryl protons could not be obtained. Improved solution phase NMR will be obtained with new, lower molecular weight samples that are currently being prepared. Elemental analysis (Galbraith Laboratories) in both cases indicates H/C ratios slightly lower than expected (0.99 and 0.97 vs calculated values of 1.20 and 1.11 for the poly(eugenol) and poly(4-allylphenol), respectively).

Initial efforts to produce well-characterized -C-C-C- polymers have used the following reaction sequence:



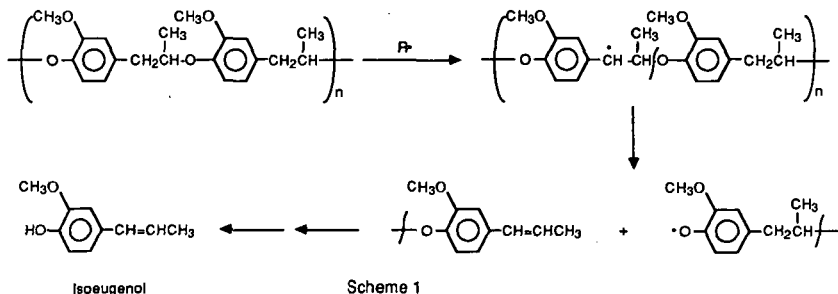
The α,α' -dibromo-*p*-xylene (V) was treated with the monoanion of dithiane (VI) in THF at -50° to -30°C . The product (VII) was characterized by TLC and NMR and found to be consistent with the anticipated structure. The dianion from VII was treated with the dibromide (V) at low temperatures for 3 hours and thereafter at room temperature for 15 hours. The THF-soluble fraction showed a polymer of MW ~ 2500 . Desulfurization of the THF-soluble portion was effected using Raney Ni and the product was exhaustively extracted to yield a polymer of MW ~ 1500 . Elemental analysis gave C = 83.86% and H = 8.7%, indicating an H/C ratio of 1.24 (as compared with an expected ratio of 1.11).

Polymer Characterization by Pyrolysis-FIMS

As with the elemental and NMR analyses, the Py-FIMS characterization of the poly(eugenol) and the poly(4-allylphenol) is appropriately described as consistent with, but not conclusive evidence of, the desired structures. Since the FIMS characterization of a material that is not volatile under high-vacuum conditions involves programmed-temperature heating to pyrolytically generated volatiles that are then mass spectrometrically analyzed, it constitutes a thermal conversion experiment that bears relevance to coal liquefaction or pyrolysis. Therefore the Py-FIMS results will be discussed in some detail.

The Py-FIMS spectra of the poly(eugenol) and the poly(4-allylphenol) are shown in Figures 1 and 2. The spectra are relatively simple and are dominated by C_1 - to C_3 -phenols or dihydroxybenzenes (catechols), and, in the case of the poly(eugenol), by an ion corresponding to the monomer (m/z 164). These products are all to be expected from the desired polymer structure. However, the relative amounts of the various fragments are quite unexpected, indicating either that the decomposition sequence is not as anticipated, or the polymer structure is not exactly as desired, or both.

In both cases, the sequence of oligomeric groupings commonly seen in Py-FIMS of linear polymers (7) is essentially absent. The poly(eugenol) (Figure 1) has a large peak at m/z 164, representing the monomer, but very little intensity in the vicinity of the dimer (m/z 328), and none in the vicinity of the trimer (m/z 492). The spectrum of the poly(4-allylphenol) is even more pronounced in this regard: there is only moderate intensity at the monomer (m/z 134) and essentially none at the dimer and trimer masses (268, 402). The ten-fold decline in intensity of the dimer relative to the monomer, and the total absence of any ion intensity corresponding to the trimer is highly unexpected for a linear polymer that cannot unzip and is thus limited to scission by random attack on its linkages. The principal expected bond scission pathways shown below for the case of the eugenol polymer should occur randomly along the polymer chain and would result in a whole sequence of oligomers, as has been reported in the pyrolysis of other linear polymers.(7)



Along with the absence of higher oligomers, Figures 1 and 2 also show that each polymer yields substantial amounts of several alkylated dihydroxybenzenes and phenols, respectively. In the case of poly(eugenol), the C_1 - and C_2 - dihydroxybenzenes are of comparable abundance to the monomer itself. In the case of the poly(4-allylphenol), C_1 - and C_2 - phenols are about ten times as abundant as the monomer. In both cases, the sum of C_1 -, C_2 - and C_3 - phenols is substantially greater than the intensities of the monomers themselves.

Examination of the temperature dependence for evolution of the major peaks in Figures 1 and 2 suggests there are separate production routes for the monomers and the more highly fragmented phenolics, at least in the case of the poly(eugenol). Figures 3 and 4 show the abundance of the individual peaks as a function of temperature for the two polymers. In the case of poly(4-allylphenol) (Figure 3), the monomer and the C₁-phenol evolve at similar temperatures. On the other hand, in the case of poly(eugenol) (Figure 4), there is substantial evolution of the monomer (164) well below 300°C, while the methyl catechol (124) does not peak until about 400°C.

Preferred evolution of the monomers at lower temperatures is consistent with the expectation (1-3,8) that depolymerization results from H-abstraction--β-scission chain processes, as depicted above in Scheme 1. The C₁- to C₃-phenols and catechols, on the other hand, do not have easily identifiable chain routes, and would be expected to be rapidly evolved only at higher temperatures. Monomer evolution is expected to be more facile for poly(eugenol) because the methoxy group decreases the strength of the phenoxy-carbon bond in the -O-C-C- linkage by about 4 kcal/mol (9, 10). All other things being equal, this decrease in bond strength would be expected to decrease by about 150°C the temperature at which an equivalent decomposition rate is observed. As Figures 3 and 4 show, the peak of monomer evolution in poly(eugenol) is at least 150°C lower than for poly(4-allylphenol). This result may have bearing on the as-yet unresolved question (8) of whether phenyl phenethyl ether-type structures are a class for which concerted decomposition in a retro-ene process is competitive with the free radical chain process shown above (Scheme 1).

The mode of formation of the C₁- to C₃-catechols and phenols is even more puzzling than the oligomer distribution. Possible routes to the C₁- to C₃-catechols could involve initial methyl-phenoxy cleavage, as the homolysis of the ca. 61 kcal/mol methyl-O bonds becomes rapid in the vicinity of 400°C. However, this suggestion is not consistent the fact that the yield of C₁- and C₂-phenolics, is actually greater for the poly(4-allylphenol), which has no methoxy group, nor with the fact that the evolution of methylphenolics reaches its maximum at about the same temperature for both the poly(eugenol) and the poly(4-allylphenol).

Liquefaction of -O-C-C- Polymers

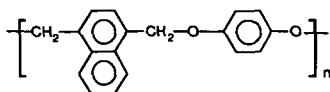
The batch microautoclave liquefaction results for poly(eugenol) and poly(p-allylphenol), and for comparison, the results for a weakly linked (-O-C-) polymer and a sample of the Argonne Zap Lignite are shown below.

PRODUCT YIELDS^a IN THE LIQUEFACTION OF MODEL POLYMERS

Sample	Hexane-Solubles	Toluene-Solubles	Pyridine-Solubles	Toluene-Insolubles	Pyridine-Insolubles	Gas
Poly(eugenol)	27	66	93	27	0	8
Poly(4-allylphenol)	1	52	96	44	0	5
Polymer VIII	85	96	100	4	0	3
Zap Lignite	14	28	46	62	50	5

^a The liquefaction tests were performed in a microautoclave reactor, using 9,10-dihydrophenanthrene as the solvent. The reactor was purged and sealed under N₂, and then immersed in a sand bath at 400°C for 30 minutes.

^b Polymer VIII is a linear polymer having the structure:



The hexane- and toluene-soluble conversions of the two -O-C-C- linked polymers are in the same order as the Py-FIMS volatilities (53 and 28%, respectively for the poly(eugenol) and the poly(4-allylphenol). They are substantially harder to convert than the weakly bonded Polymer VIII, but, in the case of the poly(eugenol), easier to convert than low-rank coal. The similarities and differences will be further considered in the Discussion Section.

DISCUSSION

The fact that the pyrolysis products are dominated by lower oligomers and smaller fragments does not, by itself, indicate whether the crosslinks were pre-existing or were generated in the course of the thermal treatment. This question is of course central to both the characterization of the original polymers, and also to an understanding of their behavior under liquefaction and other conversion conditions. Comparison of the conversion of the two -O-C-C- linked polymers with the "conversion" of other three-atom-linked models, including phenyl phenethyl ether itself, shows the apparent rate of polymer conversion to be somewhat slower than expected. Gilbert and Gajewski report (2) apparent rate parameters for phenyl phenethyl ether decomposition that correspond to a half-life at 400°C of about two hours. Considering that the linkages are somewhat weaker in both poly(4-allylphenol) and poly(eugenol) (5,9), and that many fewer than half the linkages need to be broken to make either of these polymers, if linear, fully soluble in toluene certainly supports the other indications of significant crosslinking at some stage. We are presently preparing additional batches of the poly(4-allylphenol) with phenol added during the synthesis to purposely terminate the growing polymer chains at a molecular weight level well below one million.

In general, the behavior of these two polymers is similar to the behavior of other polymeric models that are either crosslinked to begin with or are easily crosslinked during conversion and to the behavior of low-rank coals themselves, as previously discussed by Solomon and coworkers (7, 11-13). A high degree of crosslinking results in cleavage to free, and hence volatile, fragments of mainly small units, rather than large segments of a linear polymer chain. In addition, the high yields of the dihydroxybenzenes and the cresols are specifically quite similar to products generated during the pyrolysis (or liquefaction) of lignites and subbituminous coals (11-13).

Specifically, the poly(eugenol): (1) has a linkage known to be highly reactive; (2) begins to produce some monomer at temperatures lower than 200°C; (3) is nevertheless rather hard to fully convert to soluble or volatile products; and (4) has as its most abundant pyrolysis products those same alkylated catechols that tend to dominate the pyrolysis products of lignites and subbituminous coals. In other words, it bears a rather curious similarity to low-rank coals, given the limited range of structures in the original polymer. Thus it appears that these polymeric models containing -O-C-C- linkages may represent appropriate structures for use in determining the chemical details (and therefore what controls) the facile retrograde reactions of low-rank coals.

ACKNOWLEDGEMENTS

The authors wish to acknowledge the support of the U.S. Department of Energy under Contract No. DE-AC22-88PC88814.

REFERENCES

1. Poutsma, M. L.; Dyer, C. W., *J. Org. Chem.*, **1982**, *47*, 4903.
2. Gilbert, K. E.; Gajewski, J. J., *J. Org. Chem.*, **1982**, *47*, 4899.
3. Gilbert, K. E., *J. Org. Chem.*, **1984**, *49*, 6.

4. Klein, M. T.; Virk, P. S., *Ind. Eng. Chem., Fundam.*, **1983**, *22*, 35.
5. McMillen, D. F.; Golden, D. M. "Hydrocarbon Bond Dissociation Energies," *Annu. Rev. Phys. Chem.*, **1982**, *33*, 497.
6. Pedley, J. B.; Naylor, R. D.; Kirby, S. P., *Thermochemical Data of Organic Compounds*, 2nd Ed., Chapman and Hall, New York, 1986.
7. Squire, K. C.; Solomon, P. R.; Carangelo, R. M.; DiTaranto, M. B., *Fuel*, **1986**, *65*, 833.
8. Poutma, M. L., "A Review of Thermolysis Studies of Model Compounds Relevant to Processing of Coal," Report ORNL.TM-10637, Oak Ridge National Laboratory, 1987.
9. Suryan, M. M.; Kafafi, S. A.; Stein, S. E., *J. Am. Chem. Soc.*, **1989**, *111*, 1423.
10. Benson, S.W., *Thermochemical Kinetics*, 2nd ed., John Wiley and Sons, Inc., New York, 1976.
11. Serio, M. A.; Solomon, P.R.; Carangelo, R. M., *Am. Chem. Soc. Div. Fuel Chem. Preprints*, **1988**, *33(2)*, 295.
12. Deshpande, G. V.; Serio, M. A.; Solomon, P.R., *Am. Chem. Soc. Div. Fuel Chem. Preprints*, **1988**, *33(2)*, 310.
13. Solomon, P. R.; Serio, M. A.; Deshpande, G. V.; Kroo, E., "Crosslinking Reactions during Coal Conversion" accepted for publication in *Energy & Fuels*, **1990**.

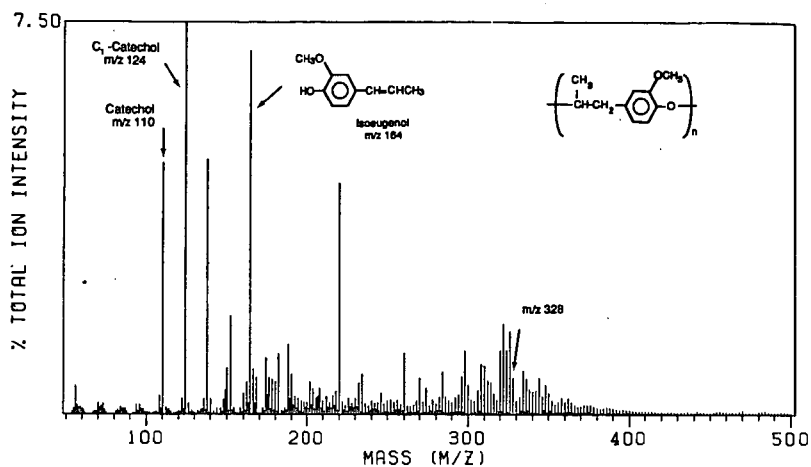


Figure 1. Pyrolysis-FI mass spectrum of poly(eugenol).

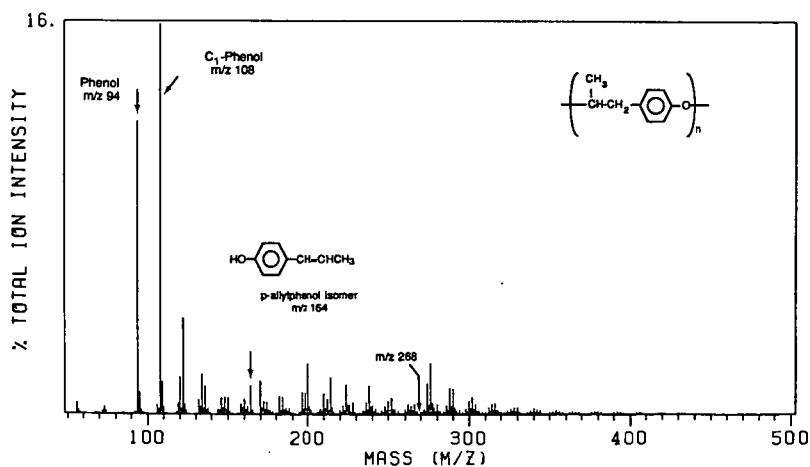


Figure 2. Pyrolysis-FI mass spectrum of poly(p-allylphenol).

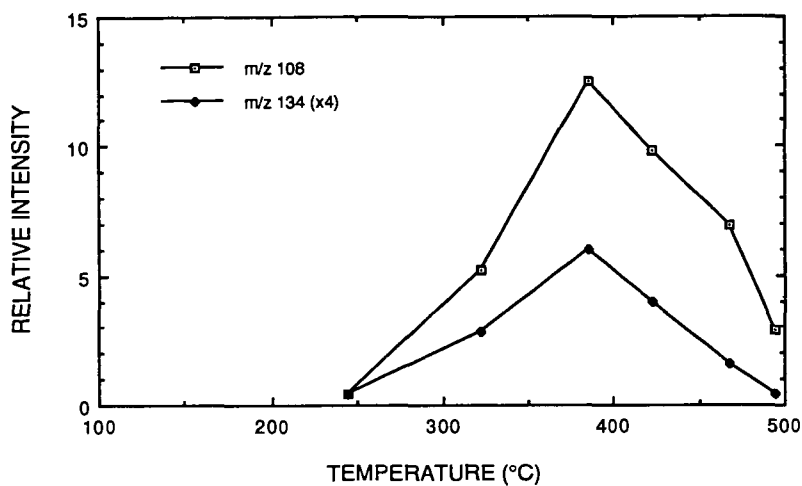


Figure 3. Thermal evolution of cresol and monomer from poly(4-allylphenol).

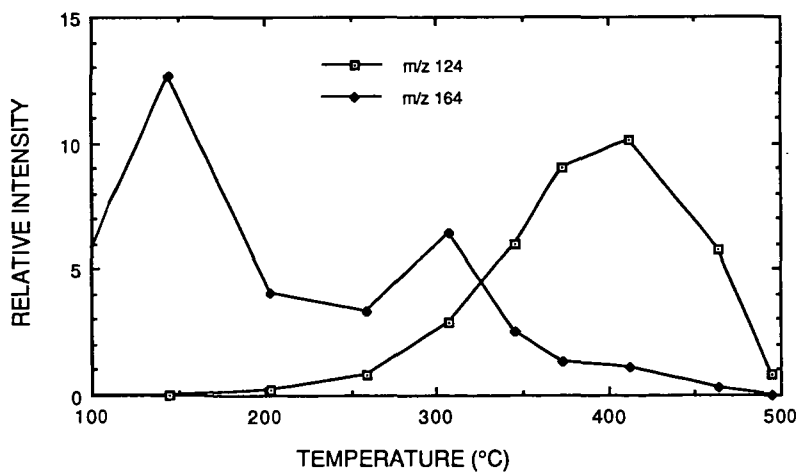


Figure 4. Thermal evolution of methyl dihydroxybenzene and monomer from poly(eugenol).

HYDROQUINONE COPOLYMERS: MODELS FOR RETROGRADE REACTIONS IN LIQUEFACTION PROCESSING

E. S. Olson, R. K. Sharma, L. J. Radonovich, Jr., M. J. Heintz, and J. W. Diehl
University of North Dakota, Energy and Environmental Research Center
Grand Forks, North Dakota 58202

The identification of structures responsible for retrograde reactions is a high priority research objective in coal liquefaction. Interest has focused on the cleavage of benzyl aryl ethers and subsequent polymerization of the fragments. In our work, the reactions of the polyethers prepared by reaction of bis(bromomethyl)naphthalene with hydroquinone were investigated in a tetralin system. Analysis of the products from the copolymers demonstrated that almost all of the naphthyl moieties were converted to dimethylnaphthalene, whereas the hydroquinone groups were converted to very high molecular weight macromolecules. Light-scattering studies showed that the product has a very high depolarization ratio, a property also demonstrated by coal macromolecules obtained by mild liquefaction and extraction but not by synthetic polymers, including polyphenylene oxides. Similar macromolecules were obtained in thermal reactions of benzyloxyphenol and dihydroxybenzenes in tetralin.

Key words: benzyl aryl ether cleavage, retrogressive reactions, dihydroxybenzene polymers

INTRODUCTION

Formation of char during coal liquefaction is deleterious to the process because of deposition on the catalyst as well as in the apparatus. Phenolic groups have been implicated in the retrogressive reactions that result in char formation in SRC materials (1,2); however, the nature of the condensation reaction that the phenolic substances undergo has never been precisely defined. The addition of hydrogen donors, such as tetralin, to SRC fractions with high phenolic content inhibited char formation (2). It is important to note in these studies that derivatization of the phenolic groups in the SRC with acetic anhydride resulted in higher char yields when the acetylated products were heated. The explanation for this was that the thermally labile esters readily decomposed forming phenoxy and acetyl radicals, which then abstracted hydrogen from other coal groups. Dimerization and addition reactions of the resulting radicals would result in char formation.

The thermal reactions of benzyl phenyl ether have been investigated as a model for the cleavage of the oxymethylene bridge in coal. The data from these modeling experiments is consistent with a mechanism involving homolytic cleavage of the C-O bond, forming phenoxy and benzyl radical intermediates. In a good hydrogen donor solvent such as tetrahydroquinoline, the radicals are capped and toluene and phenol are formed (3). However, when hydrogen donor solvent was not present or even in the presence of some tetralin, addition or condensation products were obtained (4).

The presence of dihydroxyarenes in coal structures and the well-known tendency of dihydroxybenzene to condense to polymers under oxidative conditions (5) suggests that retrogressive reactions of compounds containing dihydroxy or dioxy groups should be investigated under conditions typical of coal liquefaction. The initial model chosen for this investigation was the insoluble copolymer, poly(2,6-dimethylnaphthaleno-1,2-dioxybenzene). The 1,4-substituted analog was previously used in modeling coal pyrolysis and swelling studies (6,7,8). Reactions of the

copolymer and related monomers were carried out in tetralin so that we could determine whether retrogressive reactions could occur even when hydrogen donor solvent molecules are readily available.

EXPERIMENTAL

The procedure of Squires et al. (6) was used for preparation of poly(2,6-dimethylnaphthaleno-1,4-dioxybenzene). 1,2,3,4-Tetrahydronaphthalene (tetralin), hydroquinone, catechol, and 4-benzyloxyphenol were obtained from Aldrich.

The reactions were carried out in a 75-ml stainless steel reactor. The reaction vessel was charged with 2.00 g of model compound or polymer and 16 g of tetralin, evacuated, sealed, and heated in a fluidized sand bath at 420°C for 6 min with shaking. The tube was removed from the sand bath, cooled, slowly depressurized and opened. The product slurry was transferred into a centrifugation bottle by washing with hexane, and the solid product was removed by centrifugation. The hexane-soluble product was analyzed by GC/FTIR/MS.

The hexane-insoluble product was separated into tetrahydrofuran (THF)-soluble and insoluble fractions by extraction of the solid into that solvent. The THF-soluble product was sublimed at 110°C/1.2 torr for two hrs. The sublimate was analyzed by GC/FTIR/MS. The residue left after sublimation was analyzed by FTIR and ¹³C NMR in THF-d₈. Molecular weight determinations were performed by GPC and low-angle laser light scattering photometry. The THF-insoluble fraction was analyzed by FTIR.

RESULTS AND DISCUSSION

The thermal reaction of the mixture of poly(2,6-dimethylnaphthaleno-1,4-dioxybenzene) in tetralin at 420°C for 6 min resulted in extensive degradation of the copolymer. The product distribution was 6.5% THF-insoluble material, 28% hexane-insoluble, THF-soluble fraction, and 63% hexane-soluble fraction. The hexane-soluble fraction consisted mostly of dimethylnaphthalene and a small amount of solvent-derived dimers. Since the weight % composition of dimethylnaphthalene units in the copolymer is 60%, the formation of dimethylnaphthalene was nearly stoichiometric.

The THF-soluble fraction was sublimed under vacuum (110°C, 1.2 torr) to remove low molecular weight material. A small amount of hydroquinone was isolated as the sublimate. The majority of the fraction did not volatilize. The residue from vacuum sublimation was redissolved in THF, and the molecular weight was determined by low-angle laser light scattering photometry with Cabbanes factor corrections (9). Depolarization ratios were large for the set of solutions, resulting in Cabbanes factors as large as 3.61 for a 0.13 mg/ml solution. These high depolarization ratios are comparable with those obtained for coal macromolecules, which also scatter light anisotropically. Most synthetic polymers, including poly(phenylene oxide), have low depolarization ratios. The reciprocal Rayleigh plot of the Cabbanes-corrected scattering factors was nearly linear ($r^2 = .97$) with a positive slope ($A_2 = .0063$). The weight average molecular weight (M_w) was 1.92 million Da.

The high yield of dimethylnaphthalene indicates that the predominant pathway involves cleavage of the C-O (benzyl ether type) bonds. The resulting naphthylmethylene radicals are presumably rapidly capped by the hydrogen donor solvent. The fate of the oxy radical in this reaction is different than that of the phenoxy radical produced in the benzyl phenyl ether reaction. Only a portion of the oxy radicals produced from cleavage of the ether groups in the copolymer were converted to hydroquinone, while the majority were condensed to a high molecular weight material.

To further elucidate the difference between the mono and dioxybenzene systems, the thermal reaction of 4-benzyloxyphenol was carried out in tetralin under the same conditions. This model compound represents a single unit of the copolymer and was expected to give toluene from the benzyl radical as well as the reaction products from the oxyphenol radical. This reaction produced the expected toluene, the THF-insoluble fraction, and the hexane-insoluble, THF-soluble fraction. However, the amount of the THF-soluble fraction was smaller (14%) than that obtained from the copolymer. Sublimation of this fraction gave a small amount of hydroquinone. The molecular weight of the sublimation residue was 3.14 million Da. Depolarization ratios were similar to those observed for the product from the thermal reaction of the model polymer, resulting in Cabannes factors of 4.77 for the 0.12 mg/ml solution. The reaction of 4-benzyloxyphenol in tetralin has been reported previously (10), but no details concerning the product were given. The thermal reaction of methoxyphenols in tetralin were studied by Bredenberg and Ceylon (11). The yields of hydroquinone from 4-methoxyphenol were quite small, but the fate of the oxy radicals generated from this ether were not elucidated, since polymeric materials were not investigated. Similar poor recoveries of products from tetralin reactions of hydroquinone and 4-methoxyphenol were mentioned by Kamiya et al. (12).

The thermal reactions of dihydroxybenzenes in tetralin were reinvestigated to determine the nature of the products and their similarity to those from the ether reactions. The reaction of hydroquinone in tetralin at 420°C was carried out, and a hexane insoluble, THF soluble fraction containing the anisotropic polymeric product ($M_w = 0.95$ million Da) was obtained. Thus the cleavage of the phenolic O-H bond may give an oxyphenol radical which may be the same species as that produced in the ether C-O cleavage discussed above.

Catechol was also heated in tetralin at 420°C. Again, a polymeric product ($M_w = 1.97$ million) was obtained. The polymer from the catechol was also anisotropic, giving a Cabannes factor of 3.63 for the 0.14 mg/ml solution.

Infrared spectra of the THF-soluble polymers exhibit large broad hydroxyl stretching absorptions similar to coals. Bands characteristic of both phenols and aryl ethers occur at about 1200 and 1260 cm^{-1} , respectively. A small band corresponding to conjugated carbonyl is present at 1700 cm^{-1} . In addition to the aromatic C-H stretching bands, aliphatic bands are also present, probably from incorporation of tetralin into the polymer. Cronauer has previously discussed the tendency of radicals to incorporate tetralin (13). Further characterization of the polymeric materials is in progress.

Schlosberg et al. (4) have described a number of potential reactions of the benzyl and phenoxy radicals that result from homolytic cleavage of benzyl phenyl ethers. Most of these will also apply to oxy radicals produced in the cleavage in the dioxy systems. Until detailed information on the structures in the polymers is available, we obviously can not write detailed mechanisms for the polymer formation. We can, however, state the following generalizations:

- (1) The oxy radicals are more involved in the polymer formation than the naphthylmethylene or benzyl radicals produced in the homolytic C-O cleavage reactions of ethers of dihydroxybenzenes. This is shown by the recovery of most of the dimethylnaphthalene units as dimethylnaphthalene and benzyl as toluene. This contrasts with the reactivities of phenoxy versus benzyl radicals, which were approximately equal in the presence of hydrogen donor solvents (4).
- (2) The thermal reactions of dihydroxybenzenes and their ethers in tetralin result in polymeric products in contrast with the reactions of phenyl ethers that give additional by-products composed of mainly two or three rings (4,14).

The oxygen functional groups in coals undoubtedly play an important role in coal liquefaction. Although benzyl phenyl ether linkages are cleaved under relatively mild liquefaction conditions, we see from this study that some of the radicals resulting from this scission may readily condense into highly anisotropic macromolecules, even in the presence of hydrogen donor solvents.

REFERENCES

1. Whitehurst, D.D.; Mitchell, T.O.; Farcasiu, M. Coal Liquefaction, Academic Press, New York 1980, pp 207-273.
2. Walker, P.L.; Spackman, W.; Given, P.H.; Davis, A.; Jenkins, R.G.; Painter, P.C. "Characterization of Mineral Matter in Coals and Coal Liquefaction Residues," EPRI Project 366-1, AF-832, December 1978.
3. Brucker, R; Kolling, G. Brennstoff-Chemie 1965, 46, 41.
4. Schlosberg, R.H.; Davis, W.H.; Ashe, T.R. Fuel 1981, 60, 210-204.
5. Mather, S.P.; Schnitzer, M. Soil Sci.Soc. Am. J. 1978, 42, 591-596.
6. Squires, T.G.; Smith, B.F.; Winans, R. E.; Scott, R.G.; Hayatsu, R. Proc. Intern. Conf. Coal Sci., 1983, 292-295.
7. Solomon, P.R. "Synthesis and Study of Polymer Models Representative of Coal Structure," Final Report to Gas Res. Inst. for Feb. 1982 to Mar. 1983.
8. Barr-Howell, B. O.; Peppas, N.A.; Squires, T.G.; J. Appl. Polym. Sci. 1986, 31, 39-53.
9. Olson, E.S.; Diehl, J.W. First Pacific Polymer Conference, Preprints. Maui, HI, Dec. 1989.
10. Carson, D.W.; Ignasiak, B.S. Fuel, 1980, 59, 757-761.
11. Bredenber, J.B.; Ceylon, R. Fuel 1983, 62, 342-344.
12. Kamiya, Y.; Yao, T.; Oikawa, S. ACS Division of Fuel Chem., Preprints, 1979, 23 (4), 116-124.
13. Cronauer, D.C.; Jewell, D.M.; Shah, Y.T.; Modl, R..J.; Seshadri, K.S. Ind. Eng. Chem. Fundam. 1979, 18, 368-376.
14. Sato, Y.; Yamakawa, T. Ind. Eng. Chem. Fundam. 1985, 24, 12-15.

ACKNOWLEDGMENTS

This research was supported by Contract No. DOE-FC21-86MC10637 from the U.S. Department of Energy. References herein to any specific commercial product by trade name or manufacturer does not necessarily constitute or imply its endorsement, recommendation, or favoring by the United States Government or any agency thereof.

REACTIONS OF MODEL COMPOUNDS WITH SUPERCRITICAL WATER

C. C. Tsao and T. J. Houser
Chemistry Department
Western Michigan University
Kalamazoo, MI 49008

Keywords: supercritical water, model compounds, coal extraction

INTRODUCTION

The possible use of supercritical fluid extraction (SFE) of coal to obtain cleaner, more versatile fluid products is of significant interest. Some fluids have the opportunity to participate as reactants at process conditions, which may yield extracts of very different compositions than those obtained from other treatments and which will be dependent on the fluid used. Thermodynamic consideration of SFE leads to the prediction that the enhanced solubility (volatility) of the solute may be several orders of magnitude(1-3). Thus, this method combines many of the advantages of distillation with those of extraction. However, despite the interest in SFE, only a few studies have reported the basic chemistry that may be taking place during coal extraction at these conditions(4-8).

The current program is concerned with nitrogen removal from, and the rupture of carbon-carbon bonds between, aromatic rings in model compounds thought to be representative of structures found in fossil fuels. Because of the difficulty of removing heterocyclic nitrogen, experiments were initiated by extensively examining the reactivities of quinoline and isoquinoline, as well as brief examinations of the reactivities of other compounds(4). The selection of water as the fluid was based on its physical and chemical properties(9) and on the observation that a few studies of SFE of coal using water as the fluid have given encouraging results(10,11). Zinc chloride was chosen as a catalyst because of its reported catalytic activity for hydrocracking aromatic structures(12). This paper discusses the results of a study of the reactions of supercritical water (SW) with organic compounds that were found, or postulated, to be intermediates in the reaction of isoquinoline with SW. Since the isoquinoline reaction produced significant yields of ethyl benzene and o-xylene(4) it was assumed that benzylamine (BA) would be representative of the intermediate structure formed after the initial bond rupture in the heterocycle. It was found that benzaldehyde, benzylidenbenzylamine (BBA) and benzyl alcohol were intermediates in the BA-SW reaction(5), thus these are the primary subjects of the current study.

EXPERIMENTAL

The experiments were carried out in a small (47 cm³) stainless steel, batch reactor, which was not equipped for the collection of gaseous products for analysis. The reactor was loaded with about 2.00 g of an organic compound. Water (10 ml) was added for the SW experiments to produce the desired pressure at reaction temperature, catalysts were added as needed, then the reactor was purged with argon and bolted

closed using a copper gasket. The reactor was placed in a fluidized sand bath furnace for the required reaction time, about 15 minutes was required to reach 375°C. Following reaction, the vessel was air cooled, opened, the reaction mixture removed and the water and organic layers separated. Portions of methylene chloride solvent were used to rinse the reactor and extract the water layer. These portions were combined with the organic layer and additional solvent added to a standard volume for quantitative determinations made gas chromatographically using peak area calibrations from known solutions. The components for these solutions were identified mass spectrometrically.

There were certain limitations on the g.c.-m.s. determinations: Some components could not be separated completely and these are reported as a total yield of mixture using an average calibration factor. Some products are reported as an isomer of a probable structure as deduced from the molecular weight and m.s. fragmentation pattern. Finally, many of the higher molecular weight minor products could be measured only with a low degree of precision by g.c. and calibration factors were estimated.

RESULTS AND DISCUSSION

The previous study of the isoquinoline - SW reaction(4) has indicated that following the rupture of the CN bond in the 1-2 or 2-3 position, the nitrogen portion would undergo hydrolysis and decarboxylation while the carbon end was either capped directly, or shortened and capped, by hydrogen thus producing toluene, ethylbenzene or o-xylene, the major volatile products. To help substantiate this proposed sequence of reactions, the benzylamine - SW reaction was studied(5). Since benzaldehyde, benzyl alcohol and benzyldenebenzylamine ($C_6H_5CH_2N=CHC_6H_5$) were observed as intermediates in the BA - SW reaction it was necessary to determine how they contributed to the formation of the final products.

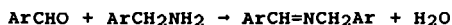
The data reported in Tables 1-4 are a small portion, but representative, of the results obtained. Ammonia was added in some experiments since it would be present in the denitrogenation of amines.

Benzyl Alcohol

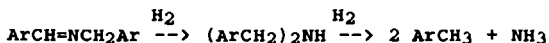
Table 1 shows that SW by itself had relatively little influence on the on the pyrolysis reaction, both giving low yields of volatile products and significant amounts of black char/tar. The added ammonia suppressed the char/tar formation, producing clear yellow solutions and significantly higher yields of volatile products. It is believed that the most important observations are: (a) that for all experiments toluene is formed in the highest yield and (b) the presence of SW does promote the formation of benzaldehyde which, as will be shown later, would lead to higher benzene yields. The second observation is consistent with other data that have shown SW capable of removing hydrogen from tetralin(4) and benzylamine (to be discussed later).

Benzyldenebenzylamine (BBA)

In this and the following sections, Ar will be used for the phenyl group (C_6H_5). The formation of BBA in the BA - SW reaction was most probably from the standard imine preparation



since benzaldehyde was also found in this reaction. The data in Table 2 show that BBA - SW reaction produces benzene and toluene in comparable yields. However, since some benzaldehyde is also produced the above reaction must be somewhat reversible. It appears that benzene and other products formed from phenyl radicals have benzaldehyde as their precursor, the evidence for which will be given later. An important point to note is that the addition of a hydrogen donor, dihydroanthracene (DHA), promotes the formation of toluene at the expense of benzene and other species which form from benzaldehyde. The following reaction sequence is a possible explanation:



Thus, it appears that rupture of the single CN bond leads to toluene while the C=N segment can be hydrolysed by the reverse of the imine formation reaction.

Benzoic Acid

It has been assumed that benzene is formed from the decarboxylation of benzoic acid although it had not been observed as an intermediate in the reactions studied earlier. The data in Table 3 show that benzoic acid does react about as expected. However, while SW appears to slow the reaction compared to pyrolysis, ammonia acts as a catalyst to produce an almost quantitative yield of benzene.

Benzaldehyde

Again it would appear that SW has relatively little effect on the pyrolysis of benzaldehyde. The data in Table 4 show that the extents of reaction and product distributions are very similar (except the benzyl alcohol yields are increased somewhat with SW) for the reactions with and without water. However, with the addition of ammonia the reaction rates are increased as well as the toluene yields. The most important observation is that the major product is benzene indicating an oxidation/decarboxylation sequence is predominant. Clearly the presence of a source of hydrogen (DHA) promotes the benzyl alcohol sequence to form toluene at the expense of benzene. To a lesser degree ammonia has a similar effect but the mechanism by which this occurs would be very speculative.

The conclusion that can be drawn is that benzene and other products formed from phenyl radicals are produced through the oxidation of benzaldehyde. However, in that process since hydrogen is produced it is possible to reduce some unreacted benzaldehyde to the alcohol from which toluene and products formed from benzyl radicals are obtained, with some reversibility in the oxidation/reduction part of the sequence.

Another possibility is that the Cannizzaro disproportionation is taking place which is base catalyzed. However, this would be expected to lead to equal yields of benzoic acid and benzyl alcohol or their respective subsequent products. Since the products resulting from benzoic acid are predominant it appears that SW may alter the mechanism to favor this product, possible through hydrogen removal from a benzaldehyde-water adduct.

Mechanism Considerations

The formation of biphenyl and 168 isomers (methyl biphenyls) as well as benzene demonstrate that phenyl radicals exist as intermediates. The formation of bibenzyl and other 182 isomers (benzyl toluenes) and the 168 isomers as well as toluene demonstrate the presence of benzyl radicals. The previous results with bibenzyl and SW(5) show conclusively that once benzyl radicals form, they abstract hydrogen or combine with other radicals resulting in very little (if any) oxidation/decarboxylation to benzene. These results from bibenzyl in addition to those obtained from BA, BBA and BBA plus DHA lead to the following conclusions: (a) The CN bond in the reactant is necessary for the hydrolysis/oxidation sequence to be initiated. (b) If a CN single bond exists in an aromatic side chain it may rupture to form a radical that is capped by hydrogen producing an alkylated aromatic, or hydrogen can be removed to form a CN multiple bond. (c) Once formed, the CN multiple bond can undergo the oxidation/decarboxylation process. (d) These reactions are somewhat reversible. (e) Ammonia catalyzes the hydrolysis/oxidation and decarboxylation processes. (f) Finally, it must be concluded that SW can facilitate the removal or transfer of hydrogen from many reactants and intermediates as evidenced by the results of tetralin in SW(4), benzaldehyde sequence of reactions from the BA-SW reaction(5), benzamide and from benzaldehyde-SW with added ammonia (Table 4) and for many of the hydrolytic/oxidation sequences leading to the observed products to be possible.

REFERENCES

1. N. Gangoli and G. Thodos, Ind. Eng. Chem., Prod. Res. Dev., 16, 208, (1977).
2. D.F. Williams, Chem. Eng. Science, 36, 1769, (1981).
3. J.C. Whitehead and D.F. Williams, J. Inst. Fuel, 182, (1975).
4. T.J. Houser, D.M. Tiffany, Z. Li, M.E. McCarville and M.E. Houghton, Fuel, 65, 827, (1986).
5. T.J. Houser, C.C. Tsao, J.E. Dyla, M.K. VanAtten and M.E. McCarville, Fuel, 68, 323, (1989).
6. M.A. Abraham and M.T. Klein, Ind. Eng. Chem. Prod. Res. Dev., 24, 300, (1985).
7. S.H. Townsend and M.T. Klein, Fuel, 64, 635, (1985).
8. J.R. Lawson and M.T. Klein, Ind. Eng. Chem. Fund., 24, 203, (1985).
9. E.U. Frank, Endeavour, 27, 55, (1968).
10. G.V. Deshpande, G.D. Holder, A.A. Bishop, J. Gopal and I. Wender, Fuel, 63, 956, (1984).
11. V.I. Stenberg, R.D. Hei, P.G. Sweeny and J. Nowak, Preprints, Div. Fuel Chem., Am. Chem. Soc., 29(5), 63, (1984).
12. S.S. Salim and A.T. Bell, Fuel, 63, 469, (1984).

Table 1 Benzyl Alcohol - SW Reaction^a

Water Pressure (psi)	0	3870	3870	3870
Added NH ₃ (Molar)	0	0	2M	6M
Volatile Products ^b (%Yield)				
Benzene	2.8	2.6	19	21
Toluene	24	20	42	44
Benzaldehyde	0	6.0	9.5	5.5
Biphenyl	0.1	0	2.3	2.6
168 Isomers	3	3	4	5
182 Isomers	8	11	2	2
DHP/Stilbene	0	0	1.6	1.4
Benzylidenebenzylamine	-	-	1.2	1.6
Above 190	8	-	1	3

a. All experiments were at 400C for 3 hrs, all extents of reaction were about 100% and the two experiments without ammonia gave black tarry products, the others gave clear yellow solutions.

b. The numbers represent molecular weights of mixtures, DHP is dihydrophenanthrene.

Table 2 Benzylidenebenzylamine - SW Reaction^a

Time(h)	1	3	6	9	3	3
Additive	0	0	0	0	6M NH ₃	2g DHA
Volatile Products ^b (%Yield)						
Benzene	22	29	35	34	28	11
Toluene	24	26	28	29	29	54
Benzaldehyde	22	11.0	3.4	2.0	3.1	0
Benzyl alcohol	2.8	2.4	0.2	0.1	0.4	0
Benzamide	0.6	0.4	0	0	0.5	0
Biphenyl	4.1	6.4	7.3	7.2	4.2	0.4
168 Isomers	4	6	7	7	5	-
Fluorene	0.1	0.4	0.6	0.8	0.4	-
Bibenzyl	2.7	2.6	2.0	1.9	3.4	-
Benzophenone	1.3	1.9	1.0	0.8	1.2	-
182-196 Mixture	4	4	2	2	2	-
Above 200	6	6	8	8	15	-

a. All experiments were at 400C and about 3870 psi water pressure. The extents of reaction were all above 95%. All solutions were clear.

b. The numbers represent molecular weights of product mixtures.

Table 3 Benzoic Acid - SW Reaction^a

Time(h)	3	4	4
Water Pressure(psi)	0	3870	3870
Added NH ₃	0	0	2 M
% Reaction	95	58	100
Volatile Products(%Yield)			
Benzene	80	79	92
Phenol	1.5	0.4	0.1
Biphenyl	3.1	0.4	0.2

* All experiments were at 400C₄₄₆

Table 4 Benzaldehyde - SW Reaction^a

Time (h)	1 ^b	6 ^b	1	3	6	1	3	6	3	9	1
NH ₃ (M)	0	0	0	0	0	2M	2M	2M	2M	2M	6M
DHA (g)	0	0	0	0	0	0	0	0	2	2	0
% Reaction	29	76	25	53	71	73	85	93	89	99	94
Volatile Products ^c (% Yield)											
Benzene	70	54	36	49	50	32	41	44	16	18	28
Toluene	6.7	7.3	5.9	8.3	6.4	11	17	21	39	38	12
Benzyl Alcohol	1.7	0	6.8	1.2	0.9	2.1	2.8	2.5	-	-	3.4
Benzoic Acid	10	6.9	14	7.5	4.7	0	0	0	-	-	0
Benzamide	-	-	-	-	-	1.2	1.0	0.7	-	-	2.6
Biphenyl	11	14	3.4	6.1	8.3	4.8	9.2	12	-	-	3.4
168 Isomers	6	9	2	3	4	2	4	6	-	-	3
166, 180-196 Mixture	19	8	10	8	5	6	7	5	-	-	5
Benzylidenebenzylamine-	-	-	-	-	-	2.0	4.3	4.0	-	-	6.1
Above 200	1	3	<1	2	4	20	7	5	-	-	13

a. All experiments were at 400C.

b. These experiments were pyrolyses, the others had about 3870 psi water pressure.

c. The numbers represent molecular weights.

Chain Transfer During Coal Liquefaction: A Model System Analysis

Concetta LaMarca, Cristian Libanati and Michael T. Klein *
Center for Catalytic Science and Technology, Department of Chemical Engineering
University of Delaware, Newark, Delaware 19716

Donald C. Cronauer
Amoco Oil Company, Research and Development Department
Naperville, IL 60566

Introduction

Coal liquefaction is a complex set of chemical reactions involving coal and solvent that is usually summarized globally in terms of the reaction of solubility- or boiling point-defined product classes. This modelling approach is warranted because both identification and kinetics solution of the large number of elementary reactions governing coal liquefaction is formidable. Nevertheless, the number of elementary reaction families is far less than the actual number of governing elementary reactions, which permits a hybrid molecular/lumped analysis of coal liquefaction kinetics. This also allows some of the rigor of molecular chemistry to be brought to bear on the synthesis of novel coal liquefaction process concepts. The purpose of the present paper is to use a hybrid molecular/lumped analysis of coal liquefaction reaction families to suggest the possibility of optimal chain transfer solvents for the initial stages of coal fragmentation.

The liquefaction reaction families are organized in Figure 1. Bond homolysis, followed by radical capping, is a time-honored view of coal liquefaction that has recently been suggested [1] to constitute only a portion of the overall reaction set. Any coal- or solvent-derived radical can abstract hydrogen from a donor (within coal or from a solvent); these radicals can also induce cleavage of coal bonds through ipso substitution and radical-induced hydrogen transfer (RHT). Kinetically significant β -scission steps are also available to coal- and solvent-derived radicals. Radical recombination and radical addition to olefins, the reverse of bond homolysis and β scission, respectively, are also kinetically significant.

As regards coal liquefaction, steps 1-4 are desirable: they lead to molecular weight reduction. Steps 5 and 6 are undesirable, since they lead to molecular weight growth (these might be termed "primary" retrograde reactions). Increasing the rates of 1-4 relative to 5 and 6 during the initial stages of coal liquefaction would allow for better net fragmentation of the macrostructure. As developed below, this can amount to increasing the kinetic chain length during the initial stages of coal liquefaction.

The reaction families 1-6 collectively possess aspects of a kinetic chain process. Reaction 1 initiates, Reaction 2-4 (and 6) propagate, and Reaction 5 terminates a chain. The essential feature of the chain is its kinetic chain length, i.e., the rate of consumption of coal by steps 2-4 relative to that by step 1. At the condition of steady state, step 1 must be equal in rate to step 5, which is a primary retrograde reaction. As highlighted in Figure 1, a chain transfer solvent will catalyze the desirable kinetic cycle through hydrogen transfer steps, increasing the turnover of the propagation cycle by shuttling H atoms without net consumption of hydrogen; μ_2 is regenerated in the cycle. A chain transfer solvent will, by definition, have slow β -scission pathways available to μ_2 . Of course, μ_2 can terminate with itself or coal-derived radicals, and may also be less reactive than the original coal-derived radical, R , of Figure 1. Both of these factors would tend to lower the turnover or chain length, which motivates the need for quantitative kinetics analysis.

The classic Rice-Herzfeld (RH) formalism provides a convenient vehicle for the kinetics analysis of the foregoing chemistry. The reaction families of Figure 1 are organized according to the RH formalism in Figure 2, which includes unimolecular bond homolysis, bimolecular hydrogen transfer, unimolecular β scission and bimolecular termination steps for coal and coal-derived radicals. Additional bimolecular hydrogen transfer and recombination steps involve the chain transfer solvent. Note that the propagation cycle, i.e., the hydrogen transfer and β -scission steps, sum to include the RHT step, which is therefore implicitly included in this analysis.

In outline of the remainder of this communication, kinetics analysis of the scheme of Fig. 2 is aimed at resolving the attributes of solvents that will enhance turnover of the propagation cycle, i.e., the kinetic chain length. This analysis will also show, as suggested by McMillen [1], the existence of a solvent of optimal C-H bond strength. In particular, the solvent with the most easily donatable hydrogen is not the best liquefaction

* Corresponding author.

solvent. We will show that the intrinsic chemistry that controls the catalytic effect of the chain transfer solvent is determined by the difference in reactivities of the coal- and solvent-derived radicals.

Analysis

Kinetics analysis of the steps of Figure 2 is phrased in terms of the RH transformation of reactant ($A_1 = \mu_1 H$) through free-radical intermediates β_1 and μ_1 to products $\beta_1 H$ and Q_1 . Chain transfer occurs through the addition of A_2 ($\mu_2 H$), which can donate hydrogen to β_1 , or to μ_1 in the case of slow β scission. The thus-derived μ_2 radical can abstract hydrogen from A_1 or terminate with another radical. Individually, A_2 is stable and, in particular, μ_2 does not have a kinetically significant β -scission path. This results in no net consumption of the catalyst A_2 .

The long-chain rate of consumption of A_1 ,

$$r_{A_1} = k_{11}A_1\beta_1 + k'_{21}A_1\mu_2 - k'_{12}A_2\mu_1 \quad (1)$$

can be written in terms of observable species' concentrations by invoking the pseudo-steady state approximation on radical concentrations. The β_1 and μ_1 balances provide the concentrations μ_1 and μ_2 in terms of β_1 . The equality of initiation and termination rates then provides the final information needed to express β_1 (and, thus, μ_1 and μ_2) in terms of A_1 , A_2 and the rate constants for elementary steps.

The thus-derived rate expression for the pyrolysis of A_1 in the presence of a chain transfer solvent (A_2) is:

$$r_{A_1}(A_1, A_2) = \left(\frac{\alpha_1 A_1}{k_t} \right)^{\frac{1}{2}} \frac{k_{11}A_1(1 + \hat{k}'\theta'S_2)}{D^{\frac{1}{2}}} \quad (2)$$

where,

$$D = (1 + \hat{k}'S_2(\gamma_3 + \gamma_5\hat{k}'S_2) + M_1(1 + \hat{k}'\theta'S_2)(\gamma_1 + \hat{k}'S_2(\gamma_3\phi' + \gamma_4 + 2\gamma_5\phi'\hat{k}'S_2) + M_1^2(1 + \hat{k}'S_2)^2(\gamma_2 + \hat{k}'\phi'S_2(\gamma_4 + \gamma_5\hat{k}'\phi'S_2))) \quad (3)$$

In Eqs. 2 and 3, $M_1 = k_{11}A_1/k_t$, $\hat{k}' = k_{12}/k'_{21}$, $\theta' = k'_{21}/k_{11}$, $\phi' = k_{12}/k'_{12}$, $S_2 = A_2/A_1$ and γ_i is a termination rate constant relative to that for β_1 self-termination.

The influence of the chain transfer solvent A_2 is emphasized by considering the enhancement $E_1 = r_{A_1}(A_1, A_2)/r_{A_1}(A_1)$ of the rate of consumption of A_1 caused by the addition of A_2 . Recognizing $r_{A_1}(A_1)$, the rate in the absence of a chain transfer additive, to be:

$$r_{A_1}(A_1) = \left(\frac{\alpha_1 A_1}{k_t} \right)^{\frac{1}{2}} \frac{k_{11}A_1}{(1 + (\gamma_1)M_1 + (\gamma_2)M_1^2)^{\frac{1}{2}}} \quad (4)$$

E_1 reduces as:

$$E_1 = \frac{(1 + \hat{k}'\theta'S_2)(1 + (\gamma_1)M_1 + (\gamma_2)M_1^2)^{\frac{1}{2}}}{D^{\frac{1}{2}}} \quad (5)$$

The chain transfer solvent therefore effects rate enhancement through modified rates of chain propagation (\hat{k}' , θ' , S_2) and chain termination ($\gamma_1, \gamma_2, \dots, \gamma_5, \phi'$). θ' indicates the ease of H abstraction from A_1 by μ_2 and β_1 radicals, and \hat{k}' is a cross-coupling parameter which compares the propensity of β_1 radicals to abstract H from A_2 with that of μ_2 radicals to abstract H from A_1 . ϕ' describes relative time constants for H abstraction from the shuttle molecule by μ_1 and β_1 radicals, respectively.

Application of Eq. 5 to coal liquefaction reaction families suggests several chemistry-driven simplifications. In many cases β scission is fast relative to H abstraction ($M_1 \rightarrow 0$) which permits the simplification of Eq. 5 to:

$$E_1 = \frac{(1 + \hat{k}'\theta'S_2)}{(1 + \hat{k}'S_2(\gamma_3 + \gamma_5\hat{k}'S_2))^{\frac{1}{2}}} \quad (6)$$

In this instance β_1 and μ_2 are the most abundant reaction intermediates. For the reasonable limiting case of equal termination rate constants save the statistical factor of 1/2 for self collision, the denominator simplifies to a perfect square and allows E_1 to be written as:

$$E_1 = \frac{(1 + \hat{k}'\theta'S_2)}{(1 + \hat{k}'S_2)} \quad (7)$$

Thermochemical Constraint

Further inspection of the controlling dimensionless groups \hat{k}' and θ' shows them to be relative rate constants for a family of hydrogen abstraction reactions. The Evans-Polanyi relation $E^* = E_0 + \alpha \Delta H_R^1$ for exothermic reactions (EXO) [2] should then provide a reasonable estimate of E_1 in terms of reaction enthalpies and, ultimately, comparative bond strengths [3-9]. The dependence of these dimensionless groups on the relevant bond strengths is illustrated in Table 1, where θ' is shown to be a function of $d_{\beta_1-H}^0$ and $d_{\mu_2-H}^0$ and \hat{k}' a function of $d_{\beta_1-H}^0$, $d_{\mu_2-H}^0$ and $d_{\mu_1-H}^0$.

Eqs. 6 and 7 for E_1 and the expressions in Table 1 for θ' and \hat{k}' , allow illustration of the dependence of E on $d_{\mu_2-H}^0$, $d_{\beta_1-H}^0$, and $d_{\mu_1-H}^0$. For a model where coal species are lumped as pseudo component 1, and with the chain transfer solvent as pseudo component 2, it is reasonable to consider $\beta_1 H$ and $\mu_1 H$ as fixed by the coal type and $\mu_2 H$ to be a design parameter. This renders E_1 dependent on $d_{\mu_2-H}^0$ and T for a given coal. This dependence is illustrated in Figure 3 for $T = 400^\circ C$ and $d_{\beta_1-H}^0 = 87$ kcal/mol, the bond strength for fission of toluene, $\beta_1 H$, into H and β_1 . Inspection of Figure 3 reveals an extremum in the dependence of E_1 on $d_{\mu_2-H}^0$. For low $d_{\mu_2-H}^0$, the easily formed μ_2 radicals are also very stable. Here $\mu_2 - H$ acts as an inhibitor and lowers the rate. At the high $d_{\mu_2-H}^0$ extreme, highly reactive μ_2 radicals are formed only with great difficulty. In the limit $d_{\mu_2-H}^0 \rightarrow \infty$ the additive acts as an inert diluent, and $E_1 \rightarrow 1$. In an intermediate regime of $d_{\mu_2-H}^0$ the enhancement $E_1 > 1$. Thus Figure 3 summarizes the homogeneous equivalent of the classic Balandin Volcano curve illustrating the principle of Sabatier.

The effect of unequal termination rate constants (Eq. 6) is illustrated in Figure 4. When, for example, μ_2 radicals terminate with one one-thousandth the rate constant of β_1 radicals ($\gamma = 0.001$), the enhancement is amplified by a factor of about 4.

Sensitivity to Parameters

Eq. 7 allows more careful delineation of the conditions for enhancement and the location of the maximum of Fig. 3. Clearly $E_1 > 1$ for $\theta' > 1$, or $d_{\mu_2-H}^0 > d_{\beta_1-H}^0$. This indicates that the formation of a less-stable μ_2 radical, relative to the β_1 radical, will increase the rate relative to neat pyrolysis. Likewise, for $\theta' < 1$, the rate will decrease. But the magnitude of the effect will depend upon the rate of forming the μ_2 radicals, as shown by the derivative of E_1 with respect to $\hat{k}'S_2$. i.e.,

$$\frac{\partial(E_1)}{\partial(\hat{k}'S_2)} = \frac{(\theta' - 1)}{(1 + \hat{k}'S_2)^2} \quad (8)$$

450

This is positive for $\theta' > 1$ and negative for $\theta' < 1$. Thus the group $\hat{k}'S$ attenuates the effect dictated by the value of θ' . Finally, the curves parametric in $d_{\mu_1-H}^0$ in Figure 3 intersect at $\theta' = 1$, which corresponds to $d_{\mu_2-H}^0 = d_{\beta_1-H}^0$, for all values of $d_{\mu_1-H}^0$.

Relevant coal model compound data are summarized in Table 2. The enhancement of dibenzyl ether (DBE), $d_{\mu_1-H}^0 = 78.85$ kcal/mol and $d_{\beta_1-H}^0 = 87$ kcal/mol) was observed in each of diphenylmethane, triphenylmethane, fluorene, dihydroanthracene, dihydrophenanthrene, and bibenzyl. The chain transfer solvents span a range of both C-H bond strengths [3-10] and termination rate constants. For example, triphenylmethyl radicals are known to be persistent due to steric hindrance to self collision. In this case, $\gamma_5 \rightarrow 0$ and $\gamma_3 \ll 1$, and therefore the effect on DBE pyrolysis is predicted by the uppermost curve of Fig. 4.

Actual coal liquefaction data are consistent with the existence of an optimal chain transfer solvent. McMillen's analysis of the coal conversion data of Curtis [11] in terms of the C-H bond dissociation energy of the liquefaction solvent is summarized in Figure 5. McMillen's observation that the 'optimal' solvent was not that which most easily donated hydrogen (low $d_{\mu_2-H}^0$) supported the hypothesis that the traditionally accepted view of coal liquefaction comprising bond scission and radical capping was incomplete. The likelihood of radical hydrogen transfer (RHT) as a mechanism for the fragmentation of strong bonds was noted. The behavior in Figure 5 is also consistent with the notion of an optimal chain transfer solvent. This suggests that the chain transfer scheme of Fig. 1 may contribute to the overall observable kinetics of coal liquefaction. Further delineation of the contributions of chain transfer, fission, RHT, etc. awaits more detailed accounting of the differences between coal and its model compounds.

¹ For endothermic reactions (ENDO) $E^* = E_0 + (1 - \alpha)\Delta H_R$

Conclusions

In summary, kinetic coupling of reaction cycles involving coal and solvent species can result in the presence of an optimal solvent for coal liquefaction. The present analysis permits qualitative prediction of this behavior using the hybrid molecular/lumped chain transfer scheme outlined in Fig. 1. Model compound data are consistent with these predictions.

References

1. McMillen, D. F., R. Malhotra, G. P. Hum and S.-J. Chang. *Energy & Fuels* **1987**, *1*, 193-198.
2. Evans, M. G. and M. Polanyi. *Trans. Faraday Soc.* **34**, 11, 1938.
3. Stein, S. E. "A Fundamental Chemical Kinetics Approach to Coal Conversion", in *New Approaches in Coal Chemistry*, Blaustein, Bockrath and Friedman, eds. ACS Symp. Ser. 169, Washington D. C., 1981.
4. Benson, S. W. *J. Chem. Ed.* **42** (9) 1965, 502.
5. Bockrath, B., E. Bittner, and J. McGrew. *J. Am. Chem. Soc.* **1984**, **106**, 135-138.
6. Benson, S. W. *Thermochemical Kinetics*, 2nd ed., John Wiley and Sons, Inc., New York, 1969.
7. McMillen, D. F. and D. M. Golden. *Ann. Rev. Phys. Chem.* **1982**, **33**:493-532.
8. Billmers, R., R. L. Brown and S. E. Stein. *Int. J. Chem. Kin.* **21**, 375-386 (1989).
9. Ogier, W. C., D. F. McMillen and D. M. Golden. *Int. J. Chem. Kin.* (1982).
10. McMillen, D. F., R. Malhotra, S.-J. Chang, W. C. Ogier, S. E. Nigenda and R. H. Fleming. *Fuel* **1987**, **66**, 1611.
11. Curtis, C. W., J. A. Guin and K. C. Kwon. *Fuel* **63** 1404, 1984.

Acknowledgment

We are grateful for the support of this work by Amoco Oil Company and the Delaware Research Partnership Program.

Table 1: Thermochemical Relationships

Dimensionless Group [D]	- RT ln D = ΔE°		
	EXO/EXO	ENDO/EXO	EXO/ENDO
$\theta' = \frac{k'_{21}}{k'_{11}}$	$[(1 - \alpha)d_{\mu_2H}^\circ - \alpha d_{\beta_1H}^\circ - (1 - 2\alpha)d_{\mu_1H}^\circ]$	$[\alpha(d_{\beta_1H}^\circ - d_{\mu_2H}^\circ)]$	—
$\hat{k} = \frac{k'_{12}}{k'_{21}}$	$[\alpha(d_{\beta_1H}^\circ + d_{\mu_1H}^\circ - 2d_{\mu_2H}^\circ)]$	$[\alpha d_{\beta_1H}^\circ - d_{\mu_2H}^\circ + (1 - \alpha)d_{\mu_1H}^\circ]$	$[\alpha d_{\mu_1H}^\circ - d_{\mu_2H}^\circ + (1 - \alpha)d_{\beta_1H}^\circ]$

Table 2: Experimental Observations of DBE Enhancement in Chain Transfer Solvents

Solvent	E	$d_{\mu_2H}^\circ$	Explanation	Conclnsions
Diphenylmethane	0.8	84±2	($\theta' = 0.57$)	$\gamma_5 \sim 0.25$
Triphenylmethane	1.5	75±4	$\gamma < 1$ due to steric hindrance ($\theta' = 0.025$)	$\gamma_5 \sim 0.0003$
Fluorene	1.3	81	$\gamma < 1$ due to steric hindrance ($\theta' = 0.33$)	$\gamma_5 \sim 0.3$
Dihydroanthracene	0.40	77±2	($\theta' = 0.077$)	$\gamma_5 \sim 0.04$
Dihydrophenanthrene	0.37	83	($\theta' = 0.47$)	$\gamma_5 \sim 2$
Bibenzyl	0.65	85±3	($\theta' = 0.69$)	$\gamma_5 \sim 1.5$

Figure 1

Coal Liquefaction Reaction Families

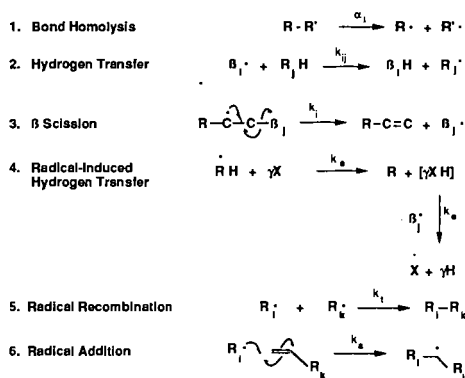
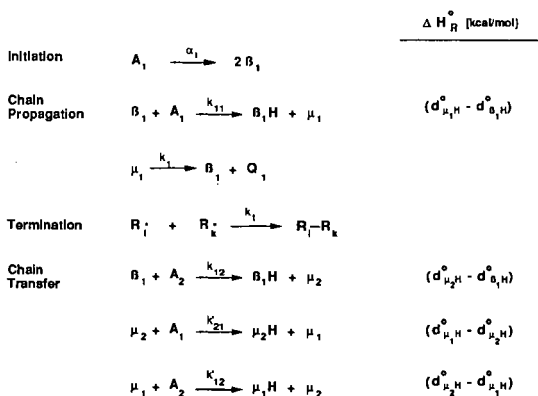


Figure 2

Rice-Herzfeld Pyrolysis Mechanism

Including Chain Transfer Elementary Steps



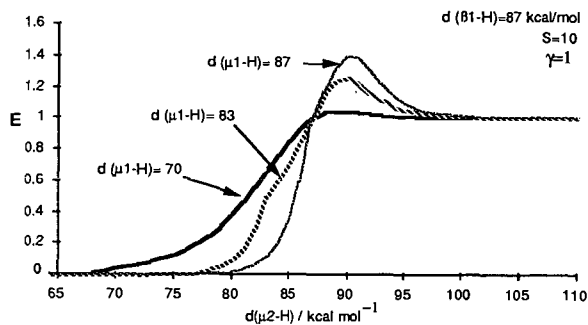


Figure 3 Rate Enhancement due to Hydrogen Transfer Solvent

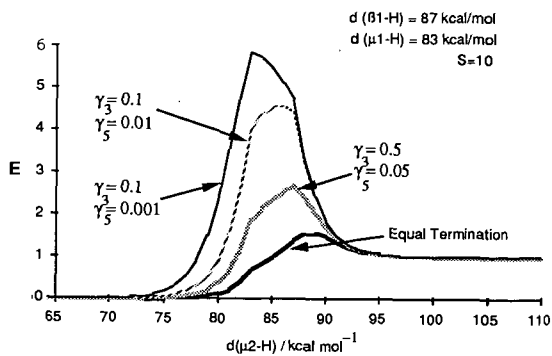


Figure 4 Rate Enhancement due to Chain Transfer Solvent:
Effect of Unequal Termination Rate Constants

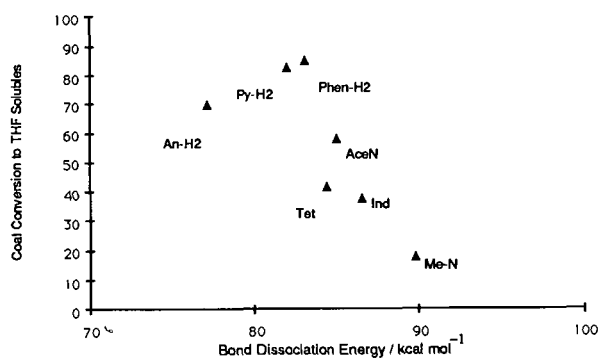


Figure 5 Coal Liquefaction Efficiency